Quaternary Structure Dynamics and Carbon Monoxide Binding Kinetics of Hemoglobin Valency Hybrids

John S. Philo, Ulrich Dreyer, and Jeffrey W. Lary
Department of Molecular and Cell Biology, The University of Connecticut, Storrs, Connecticut 06269-3125 USA

ABSTRACT The kinetics of CO binding and changes in quaternary structure for symmetric valency hybrids of human hemoglobin have been extensively studied by laser photolysis techniques. Both $\alpha^{+}\beta$ and $\alpha\beta^{+}$ hybrids were studied with five different ferric ligands, over a broad range of CO concentrations and photolysis levels. After full CO photolysis, the hybrid tetramers switch extensively and rapidly (<200 μs) to the T quaternary structure. Both R → T and T → R transition rates for valency hybrid tetramers with 0 and 1 bound CO have been obtained, as well as the CO association rates for α and β subunits in the R and T states. The results reveal submillisecond R ⇌ T interconversion, and, for the first time, the changes in quaternary rates and equilibria due to binding a single CO per tetramer have been resolved. The data also show significant α-β differences in quaternary dynamics and equilibria. The allosteric constants do not vary with the spin states of the ferric subunits as predicted by the Perutz stereochemical model. For the $\alpha\beta^{+CN}$ hybrid the kinetics are heterogeneous and imply partial conversion to a T-like state with very slow (seconds) R ⇌ T interconversion.

INTRODUCTION

There is continued interest in the properties of partially liganded intermediates in oxygen binding to hemoglobin, as well as in model systems expected to mimic the properties of such intermediates. For example, the extensive studies of various partially liganded hemoglobins by Ackers and co-workers have revealed the existence of cooperative free energy levels intermediate between those of the T and R states, a "symmetry rule" by which changes between quaternary structures depend upon the distribution of ligands within the Hb tetramer, and the existence of cooperative interactions between the α and β subunits of one $\alpha\beta$ dimer within the Hb tetramer (for a recent review see Holt and Ackers, 1995). It is hoped that further studies of such partially liganded tetramers will provide an even more detailed understanding of how ligand binding triggers the quaternary T → R transition and the detailed mechanism(s) of these phenomena (Daugherty et al., 1991; Perrella et al., 1990; LiCata et al., 1993; Huang and Ackers, 1995). One area that has not been extensively explored concerns the rates of structural and affinity transitions for partially liganded tetramers. Surprisingly, a number of studies of diliganded tetramers suggest that they have extremely slow R ⇌ T transitions, even though it is generally assumed that such slow conformational transitions do not occur during O_2 binding to Hb A. There is also conflicting evidence about the tetramer → dimer dissociation of diliganded species.

The symmetric valency hybrids with cyanide as the ferric ligand, $(\alpha\beta^{+CN})_2$ and $(\alpha^{+CN}\beta)_2$, were one of the first models for diliganded Hb. The early stopped-flow kinetic studies by Cassoly and Gibson (1972) showed that CO binding to the deoxy/cyanomet hybrids is heterogeneous, with both fast and slow binding components, with binding rates similar to those for R and T state Hb A. Surprisingly, the fast "R" component was not due to dimers, because the kinetics were essentially independent of protein concentration, and the interconversion between the fast and slow forms was extremely slow (~1 s). Further evidence for slow interconversion between the R and T structures for these cyanomet hybrids came from NMR studies (Ogawa and Shulman, 1972) and the rates of tetramer → dimer dissociation (Nagel and Gibson, 1972). Slowly interconverting quaternary structures were also suggested by studies of the aquomet forms of valency hybrids (Rollema et al., 1978).

Studies of other diliganded intermediates have also shown evidence of very slow equilibration between R and T. Both symmetric and asymmetric ferrous Hb tetramers with two CO's bound have been prepared and studied kinetically through double-mixing stopped flow by Sharma and co-workers. They report that all of these diliganded tetramers exist as mixtures of conformers in slow (seconds) equilibrium, having CO association and dissociation rates similar to those of R and T state Hb (Berjis et al., 1990; Sharma, 1988, 1989). In a detailed analysis of the symmetric forms, they also suggest that $(\alpha\beta^{CO})_2$ and $(\alpha^{CO}\beta)_2$, which are formed by rapid reduction of the aquomet/CO valency hybrids, are initially capable of rapid R ⇌ T conversions but then undergo a conformation change to a slowly interconverting form (Berjis et al., 1990). Rollema et al. (1978), who used pulse radiolysis to rapidly reduce ferric subunits in aquomet/CO valency hybrids, also suggested an initial rapid R ⇌ T interconversion followed by a change to a slowly interconverting form.

All of this evidence of slow conformational equilibria in diliganded hemoglobins is perhaps even more puzzling when compared to other information about quaternary ki-

Received for publication 8 June 1995 and in final form 10 January 1996.

Address reprint requests to Dr. John Philo, Amgen Inc., Protein Chemistry 14-2-D, Amgen Center, Thousand Oaks, CA 91320. Tel.: 805-499-5725; Fax: 805-499-7464; E-mail: jphilo@amgen.com.

Dr. Dreyer's present address is Akzo Inc., Research Laboratories Obernburg, D-8753 Obernburg, Germany.

0006-3495/96/04/1949/17 $2.00

netics. The pioneering studies of R → T kinetics by Sawicki and Gibson were fitted to a model in which the binding of each ligand reduces the R → T rate by a factor of 2.8, which implies that the diliganded tetramer has an R → T rate of $>10^3$ s^{-1} at pH 9 and $>10^4$ s^{-1} near neutral pH (Sawicki and Gibson, 1976). Other data support rapid quaternary kinetics of mono- and triliganded Hb, and a gradual slowing of the R → T rate with ligation, as predicted by both the Sawicki and Gibson model (Zhang et al., 1990; Ferrone et al., 1985; Cho and Hopfield, 1979) and a linear free energy relation model (Eaton et al., 1991). It seems very surprising that the conformational rates would suddenly fall by ~3 orders of magnitude at the diliganded level. We therefore thought it would be worthwhile to undertake a more detailed kinetic study of the symmetric valency hybrids, with the particular aim of resolving the rates of quaternary transitions.

Another important aspect of the kinetic properties of valency hybrids that has not been explored in detail is the effects of changing the ferric ligand. Earlier kinetic studies have used the cyanomet hybrids almost exclusively. Whereas a low-spin ferric subunit is believed to be a good stereochemical model for an oxy- or CO-ligated ferrous subunit, a high-spin ferric subunit is stereochemically intermediate between the ferrous deoxy and ferrous liganded states. Therefore, changing the ferric ligand on the hybrids from cyanide to a predominantly high-spin ligand like fluoride should shift the properties of the valence hybrids toward those of a singly liganded tetramer. Indeed, earlier O_2 binding (Nagai, 1977; Brunori et al., 1970; Matsukawa et al., 1981) and spectroscopic studies (Mawatari et al., 1987; Morishima et al., 1986; Banerjee et al., 1973; Mawatari et al., 1983) show that the aquo- and fluoro-met hybrids are highly cooperative in ligand binding (Hill's $n \geq 1.5$) and have a higher allosteric constant, L. By systematically varying the ferric ligand in these valency hybrids, we have been able to vary the allosteric R ⇌ T equilibrium by nearly two orders of magnitude and therefore to explore how these changes affect the quaternary dynamics and assess whether the reported slow conformational dynamics occurs only when $L \approx 1$. Moreover, changing the ferric ligand allows us to explore whether this changes only L, or also changes the R and T state CO binding properties of the ferrous subunits. By studying how the allosteric constants vary with the spin state of the ferric ligand, these data can provide a strong, detailed test of the Perutz stereochemical mechanism of cooperativity (Perutz, 1979). And by varying the ferric subunits between α and β, we can also learn more about α-β inequivalence.

Finally, we should note that although we have been discussing the properties of the valency hybrids in terms of "R" and "T" states, an additional important question is whether or not they they have ligand binding properties corresponding exactly to the R and T states of Hb A, or instead whether they may occupy an intermediate quaternary structure or affinity state and/or the recently discovered "Y" (or "R-2") liganded quaternary structure (Silva et al., 1992; Smith et al., 1991). The existence of quaternary structures intermediate between R and T has been implied by a number of techniques (Miura et al., 1987; Makino and Sugita, 1982; Miura and Ho, 1984; Shibayama et al., 1987; Marden et al., 1986), although the intermediate cooperative energy level and the symmetry rule mechanism found by Ackers and co-workers apparently do not require a third quaternary structure (LiCata et al., 1993; Smith et al., 1987).

MATERIALS AND METHODS

Preparation of valency hybrids

Human hemoglobin A_0 and its isolated ferrous α and β chains were prepared as described previously (Philo et al., 1981). The symmetric $\alpha\beta^+$ and $\alpha^+\beta$ hybrids were prepared by mixing the appropriate ferrous (CO) and ferric (aquomet) subunits using a procedure adapted from that used by Cassoly (1981). Ferricyanide oxidation was carried out aerobically at room temperature for >15 min at a heme concentration of ~1 mM. A twofold molar excess of ferricyanide was used to ensure complete oxidation of the ferric subunit, followed immediately by buffer exchange into 10 mM phosphate, 1 M glycine, 0.1 mM EDTA, pH 8 buffer using a Sephadex G-25 column in the cold. (Inclusion of EDTA in all buffers helps to improve stability of the hybrids' oxidation state.) The ferrous subunits were then added dropwise at 0°, allowed to stand for >15 min, and the mixture was then exchanged into 10 mM phosphate buffer, pH 7.0, using a Sephadex G-25 column. For separation of the hybrid from HbCO, metHb, and unrecombined subunits, this reaction mixture was applied to a 1.5 × 20 cm CM-52 column that had been equilibrated with CO-saturated 10 mM phosphate buffer, pH 7.0. This column was stepwise eluted with pH 7.3 phosphate, releasing β subunits and HbCO, followed by pH 7.5 to release the hybrid.

For preparation of the $\alpha^+\beta$ hybrid we also used an alternative method that does not require separation of α and β chains, based on the preferential reduction of the β chain of metHb by ascorbic acid (Tomoda et al., 1978a,b). A solution ~1 mM metHb in 20 mM maleate buffer, pH 6, was first flushed thoroughly with CO, and then 10 mM ascorbate was added at room temperature. After 50 min the reaction was quickly quenched by applying the solution to a Sephadex G-25 column equilibrated with 10 mM phosphate, pH 7, in the cold, followed by CM-52 ion exchange chromatography as above. The material prepared by this method behaved identically to that prepared from isolated chains.

The purified hybrids from the CM-52 column were concentrated under N_2 in an Amicon concentrator; exchanged into oxygenated 50 mM BisTris, 0.1 M NaCl, 0.1 mM EDTA buffer at pH 6.8 on a Sephadex G-25 column; further concentrated to ~400 μM [heme]; and stored frozen under liquid N_2 until needed. (We find that storage in the presence of CO gives significant reduction of the ferric subunits in less than 1 year.)

The oxidation state of the hybrids was monitored by absorption spectroscopy in the visible region. An aliquot of each hybrid prep was first converted to the carbonmonoxy/cyanomet form, and the resulting spectrum was compared to a computer-generated sum of reference spectra for the isolated carbonmonoxy and cyanomet subunits to verify the 1:1 ferrous/ferric ratio. Subsequently, the ratio of the absorbances at the α and β band peaks for this form was used as a monitor of the integrity of the hybrid stocks.

Kinetic experiments

Saturation of the hybrids with a ferric ligand other than water was obtained with 500 μM KCN, 20 mM NaN_3, 100 mM KSCN, or 200 mM NaF. The oxy/aquomet hybrid stock was thawed; the ferric ligand was added as a concentrated solution in 50 mM BisTris, 0.1 M NaCl, 0.1 mM EDTA buffer; and more buffer was added to reach the desired concentration. The sample was then briefly spun in a microcentrifuge to remove any precip-

itated material and transferred to a small tonometer placed in ice on a shaker table. The desired CO/N_2 mixture (100%, 50%, 10%, or 1% CO) was passed through a gas washing bottle containing 10 mg/ml sodium dithionite in 1 N NaOH to remove trace O_2, then through a second bottle containing buffer to scrub any gaseous contaminants from the first, and then through the tonometer and cuvette. After ~2 h of equilibration on ice, the tonometer temperature was raised to 20°C, and after another ~30 min the sample was transferred anaerobically into a water-jacketed quartz fluorescence cuvette (4 × 10 mm internally) and sealed with a serum stopper. This procedure was adequate to avoid O_2 contamination when the ferric ligand was F^-, SCN^-, or H_2O, but when the ferric ligand was N_3^- or CN^-, some traces of O_2 could be detected kinetically near deoxy/CO isosbestic points as a slow phase (0.1–1 s) due to O_2/CO exchange. Therefore, for these ligands (and sometimes for others) we added an oxygen scavenging system consisting of 0.1 units/ml glucose oxidase (Calbiochem 346385), 100 units/ml catalase (Calbiochem 219261), and 10 mM glucose. The enzymes were added after extensive gas flushing to minimize the amount of peroxide produced by the glucose oxidase. The presence of ferric ligands such as cyanide and azide inhibits the enzyme activity, but does not totally eliminate it at the ligand concentrations we used. We find that *Aspergillus niger* catalase is more resistant to this inhibition than the bovine enzyme. Control experiments verified that these nanomolar amounts of enzymes produced no interfering optical signals and that the 10 mM glucose had no effect on the kinetics. Optical spectra were recorded both before and after the kinetic experiments to monitor for protein degradation or changes in the ferric/ferrous ratio, but these samples proved quite stable. Protein concentrations were determined by conversion to the cyanomet form and by using the standard extinction of 11.0 mM^{-1} cm^{-1} at 540 nm (Tentori and Salvati, 1981). CO concentrations were based on a Henry's law coefficient of 1.32 μM/mm Hg, and all CO binding rates are expressed on a per-subunit basis.

Kinetic data were obtained by laser photolysis, using the optics of a temperature jump instrument as described previously (Philo et al., 1988), with a monochromator bandpass of ≤3 nm. For each sample, data were recorded at several wavelengths and photolysis levels. At "maximum" photolysis (see below), data for CO rebinding were recorded at 436 nm, an isosbestic point for R-T differences in the ferrous chains, and at 366 nm, where R-T difference spectra contribute significantly to the signal. Maximum photolysis data were also recorded at two CO binding isosbestic points. At the ~80 μM heme concentrations we typically used to minimize dimer formation, the absorbance at the deoxy-CO isosbestic points near 425 nm is much too high, so we utilized another set near 455 nm, where the absorbance is much lower (but the R-T differences are still significant). There are $deoxy^R$-CO^R isosbestic points at 456.5 and 458.3 nm for $\alpha\beta^+$ and $\alpha^+\beta$, respectively, and $deoxy^T$-CO^T isosbestics at 452 and 454 nm. At these isosbestic points the data at early times reflect primarily the R ⇌ T dynamics and at later times reflect ligand binding to the T or R state, respectively. Thus recording data at all these wavelengths provides a good picture of both the quaternary and CO binding dynamics.

We were unable to achieve 100% photolysis in all $\alpha\beta^+$ samples, even with pulse energies of up to 1 joule. Control in situ experiments at 436 nm comparing kinetic signals with static differences between deoxyHb and HbCO samples show that >98% photolysis was reached for all of the $\alpha^+\beta$ hybrids; the $\alpha^{CO}\beta^{+F}$, $\alpha^{CO}\beta^{+aquo}$, and $\alpha^{CO}\beta^{+SCN}$ hybrids; and HbCO. However, no more than ~93% photolysis can be obtained for $\alpha^{CO}\beta^{+azide}$ or $\alpha^{CO}\beta^{+CN}$. This difference is not due simply to too much absorption of the photolysis beam, because at 590 nm the absorbance of the predominantly low spin derivatives is actually lower. Rather, we believe this represents a true difference in quantum yield on the ~300-ns time scale of our photolysis pulses, presumably due to an increased geminate yield in these derivatives. Significant differences between α and β subunits in quantum yields and geminate recombination kinetics for both R state tetramers and the isolated subunits have been noted previously (Morris et al., 1984; Olson et al., 1987).

For all samples data were also recorded at ~1% photolysis at 436 nm, which probes ligand binding to tetramers with one CO bound, with essentially no interference from doubly photolyzed tetramers. When such data indicated significant R ⇌ T switching, data at ~10% photolysis at the CO binding isosbestics were taken as an aid to understanding the R ⇌ T rates for tetramers with one bound CO.

For the $\alpha\beta^+$ hybrid with each ferric ligand, data were obtained for at least two CO concentrations (usually 10% and 100% CO), and each of these experiments was repeated at least once. Usually at least one sample was also measured at 50% or 1% CO, and in some cases samples were studied at low protein concentration to increase the amount of dimer. Because our initial surveys showed the behavior of the $\alpha^+\beta$ hybrids to be quite similar to that of the $\alpha\beta^+$ hybrids, fewer samples of the latter were studied. In total, 58 different samples were examined to cover a range of conditions and to ensure data reproducibility.

Dimer ⇌ tetramer association studies

Dimer → tetramer association constants for several CO-saturated hybrid forms were measured by analytical large zone equilibrium gel permeation chromatography (Turner et al., 1981). Samples were applied to a thermostated 1 × 20 cm Sephadex G-100 column using a LKB 2120 peristaltic pump. The outflow of the column passed through a micro flow cell mounted in a computer-interfaced Cary 2200 spectrophotometer. The computer calculated leading edge centroid elution times from the absorbance versus time data. Elution times were converted to apparent partition coefficients, σ, using blue dextran 2000 and copper chloride solutions to calibrate the void and internal volumes. The data for σ versus protein concentration were fitted to a dimer ⇌ tetramer association model, using measured data for HbO_2 in the presence and absence of 1 M $MgCl_2$ to help calibrate the σ values for dimers and tetramers.

Kinetic data fitting

A nonlinear least-squares fitting routine was written in which the kinetic model, Scheme I (Results), was numerically integrated using the Milne predictor-corrector method with a variable step size. The integration step size was usually set to limit the integration error to a maximum of 10^{-6} × the CO saturation per step. Varying this error limit by a factor of 10 had little effect on the fitted parameters. The program could simultaneously fit up to four data sets (typically 2500 absorbance values each), at different protein or CO concentrations or at different photolysis levels, to a common set of values for l'_T, l'_R, l'_{dimer}, k_2^{RT}, k_2^{TR}, k_3^{RT}, k_3^{TR}, and $k_{4,2}$, but with separate baselines and total absorbance change for each data set. The values for l_T, l_R, and $k_{2,4}$ were taken from the literature (see Table 1). Before each iteration $k_{4,2}$ was calculated from $K_{4,2}$ and the fixed value for $k_{2,4}$. For data recorded at 436 nm the absorbance change was assumed to be due entirely to CO binding; at other wavelengths there was the option of including an additional term from R ⇌ T spectral changes. We saw no evidence for convergence on local minima, as tested by using widely divergent starting values for the parameters.

During the initial stages of fitting, the values of l'_t and l'_T were held fixed at estimates from the literature, and l'_{dimer} was set equal to l'_R. These fits established that there was little R → T switching on partial photolysis of the azidomet and cyanomet hybrids. These partial photolysis data were therefore used to obtained refined estimates of l'_R. Because there clearly is rapid R → T switching and a high allosteric constant for fully photolyzed SCN^- hybrids, the rapid CO binding phase in these hybrids is due primarily to dimers. Therefore we next used data for the SCN^- hybrids at low protein concentrations to refine the values of l'_{dimer} and found that the fitted values closely matched values we had obtained for α and β subunits. To refine l'_T we fitted the F^- and SCN^- hybrid data, which show the strongest T binding phases. The l'_T values obtained also seem to agree reasonably well with the data for these hybrids in the presence of inositol hexaphosphate (IHP), but because of the likelihood that IHP changes l'_T as well as the allosteric parameters, we chose not to directly use the data with IHP. Finally, this procedure was iterated a second time to further refine l'_R and l'_T, with l'_{dimer} held at the values for isolated subunits. These refined CO association rates, listed in Table 1, were then held fixed at the same values for all ferric ligands in subsequent data analysis.

TABLE 1 R ⇌ T rates from fits to Scheme I

Hybrid type	$10^{-3} \times k_2^{RT}$ (s^{-1})	k_2^{TR} (s^{-1})	$10^{-2} \times k_3^{RT}$ (s^{-1})	$10^{-2} \times k_3^{TR}$ (s^{-1})	$K_{4,2}$ (μM)
$\alpha\beta^{+F}$	18.9 (17.2, 20.4)	56 (16, 94)	42 (38, 45)	34 (20, 120)	2.2 (2.0, 2.5)
$\alpha\beta^{+aquo}$	8.0 (7.6, 8.6)	104 (85, 123)	4.7 (3.0, 9.0)	33 (32, 39)	1.3 (1.2, 1.5)
$\alpha\beta^{+SCN}$	[26 ± 1.5]*‡	48 (20, 103)	55 (48, 62)	30.4 (29.6, 31.0)	5.4 (5.2, 5.7)
$\alpha\beta^{+azide}$	5.1 (4.5, 6.1)	880 (850, 980)	10 (0.1, 13)	290 (80, 440)	4.1 (3.5, 6.0)
$\alpha\beta^{+CN}$	4.8§ (3.6, 7.3)	3600§ (3100, 6800)	[1]*§ [0, 10]	[300]*§	[4 ± 2]*
$\alpha^{+F}\beta$	11 (9, 13)	100 (70, 125)	3 (1, 6)	17 (14, 26)	12 (10, 14)
$\alpha^{+aquo}\beta$	7.6 (5.2, 9.3)	79 (63, 93)	2.5 (1.0, 4.8)	12 (9, 22)	[10 ± 5]*
$\alpha^{+SCN}\beta$	21 (18, 25)	140 (70, 180)	20 (12, 30)	26 (24, 37)	13 (11, 15)
$\alpha^{+azide}\beta$	5.6 (4.0, 6.5)	450 (400, 480)	1.7 (1, 7)	23 (12, 51)	[10 ± 5]*
$\alpha^{+CN}\beta$	4.2 (1.9, 4.7)	340 (280, 360)	1.3 (0.3, 6.1)	13 (6, 33)	[10 ± 5]*

For the $\alpha\beta^+$ hybrids the fixed CO association rates were $l'_T = (8 \pm 1) \times 10^4\ M^{-1}s^{-1}$, $l'_R = (5.6 \pm 5) \times 10^6\ M^{-1}s^{-1}$, and $l'_{dimer} = (4.7 \pm 0.3) \times 10^6\ M^{-1}s^{-1}$. For the $\alpha^+\beta$ hybrids these values were $(7 \pm 1) \times 10^4\ M^{-1}s^{-1}$, $(8 \pm 0.8) \times 10^6\ M^{-1}s^{-1}$, and $(5.3 \pm 0.3) \times 10^6\ M^{-1}s^{-1}$, respectively. Other fixed rates were $l_T = 0.1\ s^{-1}$, $l_R = 0.01\ s^{-1}$, and $k_{2,4} = 1.1 \times 10^6\ M^{-1}s^{-1}$. Conditions: pH 6.8, 0.05 M BisTris, 0.1 M NaCl, 0.1 mM EDTA, 20°C.
*Value held fixed during fitting.
‡R → T reaction is biphasic; value matches rate when treated as one phase (see text).
§This hybrid is heterogenous. Values listed are those for the component in rapid quaternary equilibrium, after subtracting the slow component (see text).

Probably the biggest obstacle to data reproducibility and successful fits to multiple data sets is variation in the CO concentrations by a few percent, even after lengthy equilibration in the tonometer and correction for ambient atmospheric pressure. This is less of a problem in fitting data at 10% or 1% CO, because the majority of the free CO is that released from the protein (although the protein concentration must then be known accurately). In our hands, bubbling the gas through the protein solution generally leads to variable amounts of supersaturation (as shown by control experiments with myoglobin), as well as undesirable protein denaturation. Therefore, in calculating confidence intervals for fitted rate parameters, we assumed errors of up to ±5% in the free CO concentration.

RESULTS

We have studied the kinetics of both $\alpha^+\beta$ and $\alpha\beta^+$ hybrids with five different ferric ligands, at multiple CO and protein concentrations, with full and partial photolysis, and usually at 4 or 5 different wavelengths, for a total of over 600 kinetic experiments. This large volume of data makes it difficult to even summarize the results, let alone to describe all of them in detail. Therefore we will first present some data illustrating the overall behavior we observe, and then proceed to a more detailed quantitative analysis. Because the behaviors of the two types of hybrids are generally similar, we will focus only on the results for $\alpha\beta^+$. All data were recorded at 20°C in a pH 6.8 buffer with 50 mM BisTris, 0.1 M NaCl, 0.1 mM EDTA, plus sufficient ferric ligand to saturate the ferric subunits. A pH somewhat below physiological was chosen to enhance the stability against autoxidation of the ferrous subunits, as well as to avoid the complications of the aquo-hydroxy transition in the ferric subunits. We also chose to avoid phosphate buffers and their complicating effects as allosteric modifiers.

CO binding kinetics

Fig. 1 illustrates the kinetics of CO rebinding after maximum photolysis of $\alpha\beta^+$ hybrids with different ferric ligands. These data were taken at 436 nm, a wavelength that has a large deoxy/CO difference and which is nearly isosbestic for R ⇌ T spectral differences in the ferrous subunits, so that the absorbance change should be strictly proportional to CO binding (Sawicki and Gibson, 1976). These samples were equilibrated with a 50% CO/50% N_2 mixture, giving a more than 10-fold excess of free CO over ferrous

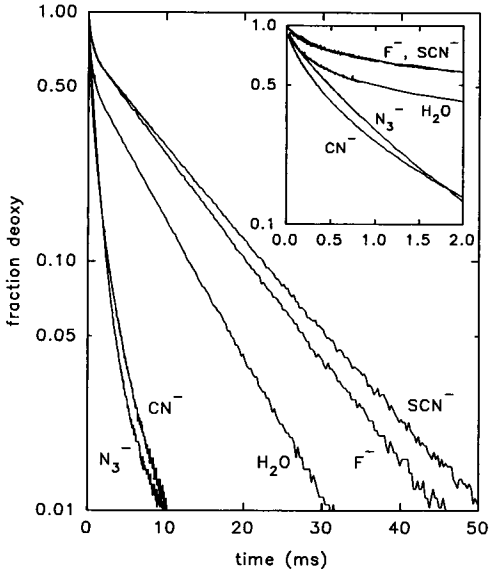

FIGURE 1 CO rebinding kinetics after maximum photolysis of $\alpha\beta^+$ valency hybrids with various ferric ligands. The kinetics were monitored at 436 nm, and the absorbance change was scaled to that for 100% photolysis. The inset shows the first 2 ms [ferrous heme] = 41–45 μM, [CO] = 500 μM (pseudo-first-order conditions for CO binding). On this semi-log plot an exponential binding phase will be linear. For the sake of clarity only every fourth data point is shown. Only about 93% photolysis can be achieved for $\alpha\beta^{+CN}$ and $\alpha\beta^{+azide}$, but >98% can be achieved for the others. Conditions: 20°C, pH 6.8, 0.05 M BisTris, 0.1 M NaCl, 0.1 mM EDTA, plus ferric ligands as needed.

heme (pseudo-first-order conditions). The data for the F^-, aquo, and SCN^- hybrids clearly show that >50% of the CO rebinding occurs as a slow exponential phase with apparent rates of 1.7–2.5 $\times$ 10^5 M^{-1} s^{-1}, i.e., rates nearly the same as the overall rate for recombination to T state Hb A. In addition, these samples show a rebinding process with a half-time of about 250 μs (more clearly seen in the figure inset), consistent with binding to R state tetramers and/or dimers, as well as small amounts of faster processes (<50 μs). The kinetics for the N_3^- and CN^- hybrids are obviously much faster and are neither monophasic nor clearly resolvable into distinct phases. The 400–500-μs half-times for the overall reaction in the N_3^- and CN^- hybrids are about twice the 210-μs half-time expected with a typical R state association rate of 6.5 $\times$ 10^6 M^{-1} s^{-1}.

Thus these full photolysis results clearly indicate the presence of T state hybrids, at least for some ferric ligands. In contrast, partial (~1%) photolysis on the same samples (Fig. 2) shows much more rapid binding, and little if any occupancy of the T state. Qualitatively, the full and partial photolysis results imply that these hybrids are, as expected, predominantly in the R state when the ferrous chains are liganded. However, they can switch to the T state when both ferrous ligands are removed and can undergo this R $\rightarrow$ T switch in <500 μs. In fact, qualitatively the data for the F^- and SCN^- hybrids closely resemble comparable experiments for Hb A.

When the samples are equilibrated with a 10% or 100% CO atmosphere, the full photolysis data for the aquo, F^-, and SCN^- hybrids continue to show prominent, resolved "R" and "T" binding phases, whose rates are proportional to [CO] (data not shown). At higher [CO], however, the relative proportion of the T phase decreases. This suggests that the R $\rightarrow$ T conversion rate is slow enough that in some tetramers CO binds before the R $\rightarrow$ T switch can occur, and this competition with CO binding limits the extent of R $\rightarrow$ T conversion. For the N_3^- and CN^- hybrids the full photolysis kinetics are nonexponential and are not resolved into distinct phases at all CO concentrations investigated, and the overall half-times are not proportional to 1/[CO].

As the protein concentration is lowered, the full photolysis data show increasing proportions of fast "R" CO binding, consistent with the fully liganded hybrids being substantially dissociated into dimers before photolysis. The extent of the concentration dependence indicates that the hybrids are more easily dissociated into dimers than is HbCO under these solution conditions.

R $\rightarrow$ T kinetics

The rapid R $\rightarrow$ T conversion can be seen more clearly in Fig. 3. These data were recorded at 456.5 nm, an isosbestic point between α(deoxy) and α(CO) for R state hybrid tetramers. At this wavelength the removal of CO by the laser pulse produces no absorbance change. Afterward we see the rapid formation of the T state, followed by its disappearance as CO rebinds and the hybrid tetramers revert to the R state. These data were recorded at a lower CO concentration to minimize the competition between CO binding and the R $\rightarrow$ T conversion.

How can we be certain that this signal is due to a change in quaternary structure, rather than a tertiary rearrangment after the rapid removal of ligand? First, the magnitude of

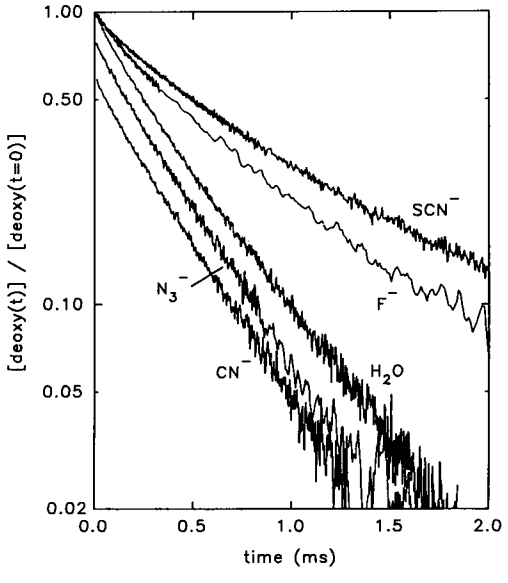

FIGURE 2 CO rebinding kinetics after ~1% photolysis. Same samples and conditions as in Fig. 1. Note that the time scale here is the same as for the inset in Fig. 1.

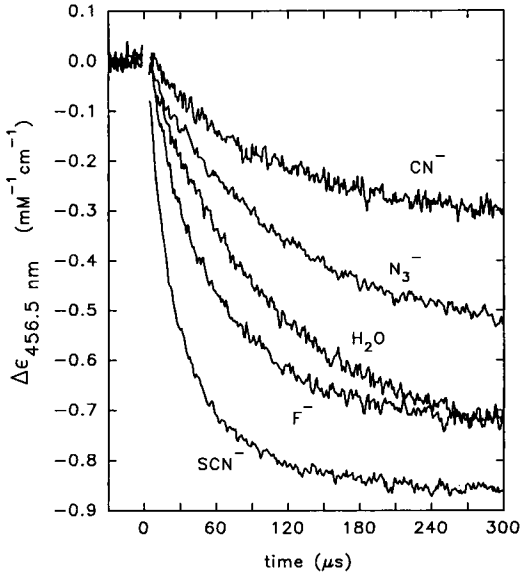

FIGURE 3 R $\rightarrow$ T kinetics after maximum photolysis. These data were measured at an isosbestic point for deoxy and CO-ligated α subunits in the R state (note the absence of an absorbance change during the photolysis pulse). Data for the first 10 μs after photolysis are obscured by scattering of the laser pulse into the photomultiplier. The absorbance returns to the preflash value at longer times, as CO is rebound. The CO concentration was reduced to 100 μM; other conditions as in Fig. 1.

this signal is strongly correlated with the extent to which CO recombination is slow after full photolysis of hybrids with various ferric ligands. More importantly, this signal disappears whenever CO recombination is essentially entirely rapid (e.g., partial photolysis of the CN^- or N_3^- hybrids, as in Fig. 2), whereas tertiary rearrangements will occur at all photolysis levels. Moreover, the magnitude and time scale of these signals are comparable to those from the R → T transition in HbCO.

Although a detailed analysis of these kinetic data (see below) does not depend on an exact assignment of these spectral changes to tertiary or quaternary effects, or to ferric or ferrous subunits, because such spectral changes have not previously been reported in valency hybrids, it is interesting to try to assign the origin of the 456.5 nm signal. Control experiments with HbCO show that the magnitude of this signal is consistent with its being predominantly due to the well-known T-R difference spectrum in the deoxy subunits (Sawicki and Gibson, 1976, 1977b; Antonini et al., 1965, 1968). Even if the R → T transition causes spin state changes in the ferric subunits, this is unlikely to constitute a major fraction of the 456.5 nm signal, because high-spin and low-spin ferric subunits have nearly equal absorbance at this wavelength. It is also possible that the R → T transition produces some signal from the ferric subunits due to spectral changes within the same spin state (i.e., spectral changes analogous to the T-R difference spectrum in deoxy Hb), especially since the absorbance of the ferric subunits is about equal to that of the deoxy subunits at this wavelength. However, such changes would presumably differ in magnitude as we change ferric ligands, whereas we do not see substantial changes in the 456.6 nm signal amplitude per T state heme. Therefore we believe most of this signal arises from quaternary effects on the deoxy hemes, but an exact assignment is not needed for interpretation of the dynamics.

When the CO concentration is raised, the rate of the initial absorbance decrease at 456.5 nm also increases, while the total amplitude decreases, because of the competition between structural/affinity interconversions and CO binding. To understand this, let us for now label the states with rapid and slow CO binding as "R" and "T," and further assume that a hybrid tetramer with one CO bound remains in the R state and/or has a very slow R → T rate. The binding of CO to either deoxy site will then effectively halt the R → T transition, and the apparent rate of this initial fast phase will be given by

$$k_{app} = k_2^{RT} + k_2^{TR} + 2 \cdot l'_R \cdot [CO], \quad (1)$$

where l'_R is the CO association rate constant for R state tetramers, k_2^{RT} is the R → T rate, and k_2^{TR} is the T → R rate for deoxy tetramers (we will use subscripts on rate constants to indicate the total number of ferrous ligands and ferric ligands bound, to facilitate comparison with the ligation states of ferrous Hb). Thus whenever $2 \cdot l'_R \cdot [CO]$ becomes comparable to the sum of quaternary transition rates, increased [CO] should both increase the apparent rate and reduce the number of tetramers able to reach the T state before CO binds. This is exactly what we observe, and this agreement is further proof that these signals are monitoring transitions related to changes in quaternary structure and/or affinity states rather than tertiary dynamics subsequent to photolysis that are not directly related to affinity transitions. The situation is similar if the tetramers with one bound CO can also rapidly switch to T, except that the factor of 2 will be absent from the rightmost term in Eq. 1. The competition between CO binding and R → T switching is much stronger in the CN^- and N_3^- hybrids than the others, and this is one reason why their CO binding kinetics are not resolved into R and T phases. This competition also significantly reduces the proportion of the T binding phase for the aquo and F^- hybrids at the higher CO concentrations (Fig. 1).

Tetramer ⇌ dimer dissociation

Because the CO binding kinetics suggested that the CO-liganded hybrids were significantly dissociated into dimers, and because others have reported essentially no protein concentration dependence in stopped-flow studies of the deoxy/CN^- hybrids (Berjis et al., 1990), we used analytical gel permeation chromatography to measure the extent of dissociation by an independent method. At the ~300 cal/mol precision for binding energies we were able to achieve, these data confirmed that the hybrids are more dissociated than is HbO_2 under these conditions. The data showed no significant difference between N_3^- or SCN^- as ferric ligands, and a somewhat greater amount of dimer for $\alpha^+\beta^{CO}$ hybrids [$K_{4,2}$ = 10 (5, 15) μM] than for $\alpha^{CO}\beta^+$ hybrids [$K_{4,2}$ = 6 (3, 10) μM] (values in parentheses are 68% confidence limits). These results are entirely consistent with the detailed kinetic analysis, and in fact the kinetic data generally give more precise values for $K_{4,2}$.

Detailed kinetic analysis

The CO binding kinetic data at different CO concentrations and both full and ~1% photolysis were simultaneously fitted to the kinetic two-state allosteric model shown in Scheme I, as described in detail in Materials and Methods. Before discussing the model in detail, we would like to emphasize that the use of this two-state model was dictated by the experimental data, and not by any preconceptions about how many quaternary structures or cooperative energy levels are accessible to these proteins, and despite an abundance of experimental evidence from other laboratories that two-state models are inadequate to describe the energetics of Hb A. The model in Scheme I is simply the minimum model we have found that is sufficient to explain our results, and for which some of the rates and equilibrium constants can be assessed independently or related to known values from the literature. There are only two affinity states in the model because we find no evidence for more; for simplicity, and by analogy with Hb A, we associate these

affinity states with particular quaternary structures, which we are labeling "R" and "T." However, labeling the conformations and parameters in the model as "R" and "T" in no way implies or assumes that they are necessarily identical to those of oxy and deoxy Hb, nor does the use of only two affinity states necessarily mean that they arise from only two quaternary structures or cooperative energy levels.

The model in Scheme I is "allosteric" in the sense that tetramer properties depend only on the quaternary conformation, and not on the number of ligands bound within that conformation. (This scheme is not in conflict with the Ackers "symmetry rule" mechanism (Holt and Ackers, 1995), in which the distribution of ligands with the tetramer is as important as the total number, because in these symmetric hybrids specifying the number of ferrous ligands also uniquely specifies their distribution in the tetramer.) Scheme I differs from kinetic formulations of the classical two-state allosteric model (Sawicki and Gibson, 1976, 1977a,b, 1978; Hopfield et al., 1971; Marden et al., 1988), however, because here we do not explictly assume that the binding of each CO reduces the allosteric constant by a factor of c.

$$\begin{array}{ccccc} & \overset{l'_T}{} & & \overset{l'_T}{} & \\ \text{hybrid}^T + 2CO & \rightleftharpoons & \text{hybrid}^T \cdot CO + CO & \rightleftharpoons & \text{hybrid}^T \cdot (CO)_2 \\ & \underset{l_T}{} & & \underset{l_T}{} & \end{array}$$

$$k_2^{TR} \downarrow\uparrow k_2^{RT} \qquad k_3^{TR} \downarrow\uparrow k_3^{RT} \qquad k_4^{TR} \downarrow\uparrow k_4^{RT}$$

$$\begin{array}{ccccc} & \overset{l'_R}{} & & \overset{l'_R}{} & \\ \text{hybrid}^R + 2CO & \rightleftharpoons & \text{hybrid}^R \cdot CO + CO & \rightleftharpoons & \text{hybrid}^R \cdot (CO)_2 \\ & \underset{l_R}{} & & \underset{l_R}{} & \end{array}$$

$$k_{4,2} \downarrow\uparrow k_{2,4} \qquad k_{4,2} \downarrow\uparrow k_{2,4} \qquad k_{4,2} \downarrow\uparrow k_{2,4}$$

$$\begin{array}{ccccc} \text{dimer} & \overset{l'_{dimer}}{} & \text{dimer} \cdot CO & \overset{l'_{dimer}}{} & \text{dimer} \cdot CO \\ \text{dimer} + 2CO & \rightleftharpoons & \text{dimer} + CO & \rightleftharpoons & \text{dimer} \cdot CO \\ & \underset{l_R}{} & & \underset{l_R}{} & \end{array}$$

$$L_2 \equiv k_2^{RT}/k_2^{TR}; \quad L_3 \equiv k_3^{RT}/k_3^{TR}; \quad L_4 \equiv k_4^{RT}/k_4^{TR}$$

$$K_{4,2} \equiv k_{4,2}/k_{2,4}$$

Scheme I

Furthermore, previous two-state kinetic formalisms have simplified the model by assuming that the binding of each CO reduces the R → T rate by a constant factor (Sawicki and Gibson, 1976, 1977b; Marden et al., 1988), but we have not imposed such a simplification here.

With regard to dimers, the model assumes that they can associate to form tetramers in the R state but cannot associate directly into T state tetramers. This seems reasonable from both a kinetic and a structural viewpoint. (Even though association of dimers into T state tetramers does not occur directly in the model, the stronger association of dimers in the T state is correctly accounted for thermodynamically through the allosteric equilibrium.) The amount of dimer present before photolysis has a strong influence on the kinetics, but the dimer ⇌ tetramer reaction rates have little influence on the data because there is very limited dimer ⇌ tetramer redistribution during the short time available. Because $k_{2,4}$ seems to vary little between hemoglobin derivatives, it was fixed at a constant value of $1.1 \times 10^6\ M^{-1}\ s^{-1}$ (Turner et al., 1981; Chu and Ackers, 1981). This model also allows the dimer to have a CO association rate differing from that of the R state tetramer. We and others (Berjis et al., 1990; Sharma, 1988, 1989; Sawicki and Gibson, 1977a) find that a small difference in CO binding rates between dimers and R state tetramers is necessary for adequate fits of the data. The data analysis was consistent with l'_{dimer} being identical to the rates measured under these conditions for the isolated ferrous subunits: $4.7 \pm 0.3 \times 10^6\ M^{-1}\ s^{-1}$ for α, $5.3 \pm 0.3 \times 10^6\ M^{-1}\ s^{-1}$ for β monomers (Philo and Dreyer, unpublished results), values that are in excellent agreement with those of Unno et al. (1991). (The β subunit in these valency hybrid dimers clearly does not show the extremely rapid CO binding seen in β_4 (Philo et al., 1988; Unno et al., 1991).) Therefore l'_{dimer} was held fixed at these independently determined values.

The partial photolysis experiments for all ferric ligands are consistent with 100% of the tetramers being in the R state before photolysis. Therefore the T state tetramer with two bound CO's does not exist at equilbrium (i.e., $L_4 \ll 1$), and we have simplified the model by setting $k_4^{RT} = 0$. The R → T signals at the isosbestic point (Fig. 3) return to the preflash value at a rate that closely matches CO binding to the T state monitored at 436 nm. This requires that k_4^{TR} is fast compared to CO binding to T. As long as this is true, the results are not sensitive to its exact value; therefore for computational convenience we set it equal to k_3^{TR}. At the relatively high protein and CO concentrations used, the slow CO dissociation rates have very little effect on the data, and fixed values of 0.1 and 0.01 s^{-1} (Sharma et al., 1976) were used for l_T and l_R, respectively.

One key question is whether the same values for l'_R and l'_T can be used for hybrids with different ferric ligands. If the R and T states are truly unique, then indeed their CO binding rates should not depend on the ferric ligand. On the other hand, the fact that for Hb A the binding rates for the first and fourth CO's appear to depend on solvent conditions suggests that there is a range of substates within each conformation, and therefore the substates might vary with the ferric ligand in the hybrids. (In our experiments it is also not possible to maintain identical solvent conditions for all of the hybrids, because the amount of ferric ligand required for saturation varies from 0 (aquo) to 200 mM (F^-). However, control experiments showed essentially no difference between partial photolysis of CN^- hybrids before and after addition of 200 mM F^- (which cannot displace the tightly bound CN^-), which demonstrates that at least the R state properties are insensitive to these differences in ionic composition.) An important result of this study is that we find that we are able to adequately represent the data for all five ferric ligands using the same fixed values for l'_R and l'_T. The fits for each ligand can be improved slightly by allowing differences among ligands, but because the improvements

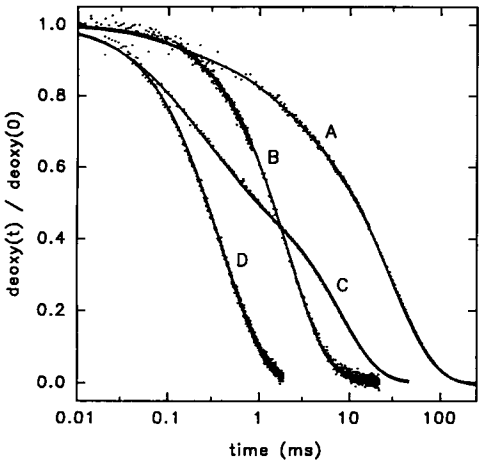

FIGURE 4 Experimental and fitted CO binding data for the $\alpha\beta^{+aquo}$ hybrid. Experimental data are shown as points (every fourth point shown), fitted data as solid lines. To accommodate both full and partial photolysis data at different CO concentrations, the binding data have been scaled relative to the initial degree of photolysis, and a logarithmic time scale is used. *A*, full photolysis, 50% CO; *B*, ~1% photolysis, 50% CO; *C*, full photolysis, 10% CO; *D*, ~1% photolysis, 10% CO. The parameters used for the fitted curves are listed in Table 1.

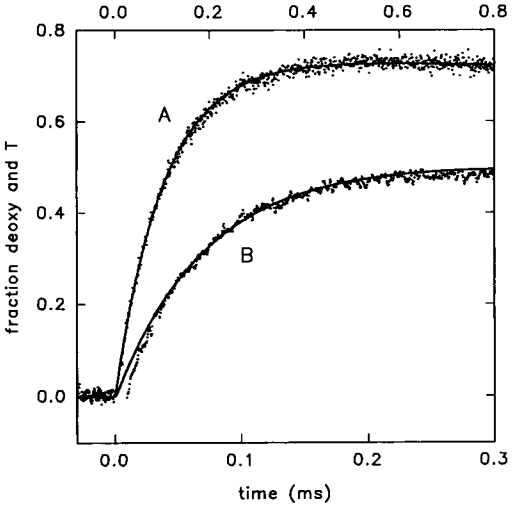

FIGURE 5 Comparison of predicted and experimental R → T kinetics. Experimental data for maximum photolysis at the 456.5 nm isosbestic point are shown as points (every fourth point shown), predicted data using the rates from Table 1 as solid lines. *A*, 10% CO/90% N_2 atmosphere, upper time scale; *B*, 50% CO/50% N_2, lower time scale. The only free parameter used in predicting these data is the magnitude of the R-T difference spectrum, which has been chosen to match the data at 10% CO. The difference between experimental and predicted data for the 50% CO data set at $t < 40$ μs is primarily due to difficulty in setting the monochromator precisely on the isosbestic point; clearly in this case the data at short times do not extrapolate to the preflash value, so the wavelength setting was slightly off the true isosbestic point (by <0.2 nm).

are small and the optimum values differ by only ~10%, we do not consider it necessary or justified to use different values for each ligand.

By fixing the CO binding rates at values from independent experiments, only the four R ⇌ T rates and $K_{4,2}$ for each hybrid need to be determined by fitting. $K_{4,2}$ was initially set within the range determined by gel permeation chromatography, but in most cases the kinetic fitting was able to determine it more accurately, and it too was allowed to vary for different hybrids. The results of these fits to the data are summarized in Table 1. In the fitting we have used only the 436 nm CO binding data. Typically, the rms error for full and partial photolysis sets at two CO concentrations is <0.4% of the CO saturation for the full photolysis sets and noise limited at ~0.014% for the partials, with systematic deviations of <3% of the total reaction.

Fig. 4 shows one example, the CO binding data and the fitted curves for $\alpha\beta^{+aquo}$. Significantly, although we have not used data recorded at the isosbestic points in the fitting, the fitted R ⇌ T rates are nonetheless generally in excellent agreement with the data at these wavelengths. In Fig. 5 we compare the predicted R → T phases for $\alpha\beta^{+aquo}$, using the fitted quaternary rates from Table 1, to the actual data at the 456.5 nm isosbestic at two different CO concentrations. The agreement is excellent, despite the fact that the only free parameter used to predict these data is the size of T-R difference spectrum at this wavelength. Fig. 5 also illustrates that rapid CO binding to the R state both increases the rate and limits the extent of switching to T at high [CO], which is the primary basis on which the analysis is able to determine k_2^{RT} from ligand binding data alone. For those hybrids that show significant R → T switching in partial photolysis experiments (e.g., the SCN^- and F^- data shown in Fig. 2), we also find excellent agreement between predictions based on the fitted values of k_3^{RT} and k_3^{TR}, and data taken at the isosbestic points at ~10% photolysis.

The fact that the rates we derive are able to correctly predict the results of independent experiments at different wavelengths, photolysis levels, and/or CO concentrations is one major reason we have confidence in the uniqueness of the fitted parameters. It is also important to emphasize that all attempts to fit these data to kinetic schemes with fewer parameters than Scheme I resulted in quite poor fits, with inconsistency between data at different photolysis levels and CO concentrations. Furthermore, we believe the parameter confidence intervals listed in Table 1 are quite conservative. Rather than basing confidence intervals only on statistical criteria for the variation in the variance of the fits (which would make them much smaller), the interval reported represents the maximum deviation found when 1) using different data sets (for example repeats of the same experiment or substituting data at 100% CO for that at 50% CO in the analysis); 2) assuming an error of ±5% in the CO concentration; or 3) varying the fixed values of l'_R or l'_T within their confidence intervals. The other fixed values in the analysis (l_T, l_R, and $k_{2,4}$) have little effect on the results; changing them by a factor of 2 typically changed the values of fitted parameters by <1%.

This quantitative analysis explains the complex CO rebinding to the azidomet hybrids in a straightforward way. While the T state is significantly occupied for these hybrids

($L_2 > 10$), their high k_2^{TR} values mean that the combined process of switching from T to R and then binding CO is comparable in rate to that of CO binding to T. Therefore the CO binding does not resolve into "R" and "T" phases, and CO binding can be quite rapid despite the relatively high allosteric constant.

In two cases the fits to Scheme I were not entirely satisfactory. For $\alpha\beta^{+SCN}$ we cannot find a unique value for k_2^{RT} that provides a consistent fit to all of the data. The fits to CO binding data at high [CO] imply a k_2^{RT} that is somewhat faster than fits to those at lower [CO] and faster than implied by the spectral changes at 456.5 nm. Significantly, for this hybrid the initial R → T phase at 456.5 nm is clearly biphasic. This can be seen in Fig. 3, where there is a slower portion of the reaction, at a rate similar to that of the F^- hybrid, tailing out to ~200 μs after an initially much faster phase. Similar biphasic R → T kinetics for Hb A near neutral pH were reported long ago by Sawicki and Gibson (1976), and we have confirmed this behavior in several buffer systems at pH < 7.5 (Philo and Lary, unpublished results). It is not clear whether the biphasic kinetics result from two conformers with different R → T rates or indicate that the conformation change is a complex, multistep process, but either possibility would explain the deviations from the model. Given this complication, we have chosen to analyze these $\alpha\beta^{+SCN}$ data with k_2^{RT} fixed at $(2.6 \pm 0.15) \times 10^4\ s^{-1}$, a value that corresponds to analyzing the 456.5 nm kinetics as a single exponential. With this value, the quality of the fits to the CO binding data at 10% and 50% CO is quite good (similar to that for the other hybrids), but at 100% CO it predicts that fewer tetramers will reach the T state than we actually observe. This same kinetic complexity may occur to a lesser extent in $\alpha^{+SCN}\beta$, $\alpha\beta^{+F}$, and $\alpha^{+F}\beta$, but for these hybrids the deviations from the model, and the biphasic character of the isosbestic point data, are only marginally significant.

Heterogeneity in $\alpha\beta^{+CN}$

A much more serious deviation from the model occurs for $\alpha\beta^{+CN}$, for which fits to Scheme I are very poor. Fig. 6 shows the ligand binding kinetics after both nearly full and 1% photolysis of $(\alpha^{CO}\beta^{+CN})_2$. The marked difference between full and partial photolysis clearly demonstrates quaternary switching, and the full photolysis data are markedly biphasic. The majority of the material binds CO at a rate ~2 times slower than for partial photolysis, while ~25% rebinds at a much slower rate, similar to that of the slow phase for $\alpha\beta^{+aquo}$. It is the presence of this slow component that causes the later stages of CO binding to this cyanomet hybrid to be slower than that for the azidomet hybrid (see Fig. 1). No such slow binding component is seen at 1% photolysis. Fig. 7 shows full photolysis data recorded at the 456.5 nm deoxy R ⇌ T isosbestic point. At early times the rapid formation of a component with a T-like spectrum is seen, consistent

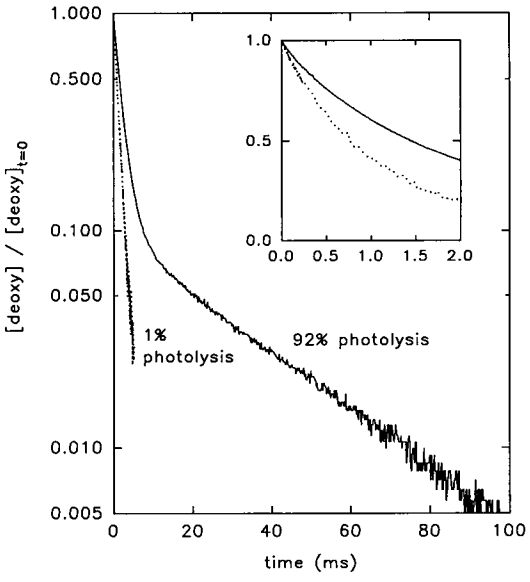

FIGURE 6 CO binding kinetics for the $\alpha\beta^{+CN}$ valency hybrid, observed at 436 nm. ——, data for 92% photolysis; · · · ·, data for 1% photolysis. This wavelength is nearly isosbestic for R-T differences, and the absorbance changes directly reflect CO binding. The ordinate has been normalized to the value immediately after photolysis to facilitate comparison of the different photolysis levels. The inset shows the first 2 ms more clearly. Only 92% photolysis can be achieved for this sample, even with a long photolysis pulse (300 ns) and up to 1 J energy, apparently because of extensive geminate recombination. Sample conditions as in Fig. 3. An oxygen scavenging system with glucose oxidase, catalase, and 10 mM glucose is also present.

with a moderately rapid R→T rate. The disappearance of this T-like component as CO rebinds is markedly biphasic. These results suggest that the major portion of the protein is in a rapid R ⇌ T equilibrium, with a T → R rate high enough that its overall CO binding is only somewhat slower than the R rate (i.e., behavior similar to that of the azidomet hybrids), while a smaller "T locked" portion has much slower T → R rates.

The presence of this slow binding component is not due to contamination with deoxy Hb, because it is not seen when azide is substituted for cyanide as the ferric ligand. This behavior is also not due to lack of saturation with cyanide, because it does not change when more cyanide is added, and it is absent when IHP is added. These observations, plus the fact that this heterogeneity of allosteric rates is present to the same extent in different protein preparations, but is not present when the same protein is combined with other ferric ligands, together strongly suggest that it is an intrinsic property of this hybrid. A similar "T-locked" state may occur to a small extent (≤3% of the total reaction) for $\alpha\beta^{+CN}$, $\alpha^{+azide}\beta$, and $\alpha\beta^{+azide}$ under these solution conditions, but the fraction is so small it is hard to be certain whether it exists.

It is important to recall that earlier stopped-flow kinetic studies of the cyanomet hybrids showed biphasic binding to two conformations not in rapid equilibrium. Our results for $\alpha\beta^{+CN}$ agree quite well with the rates seen in these earlier

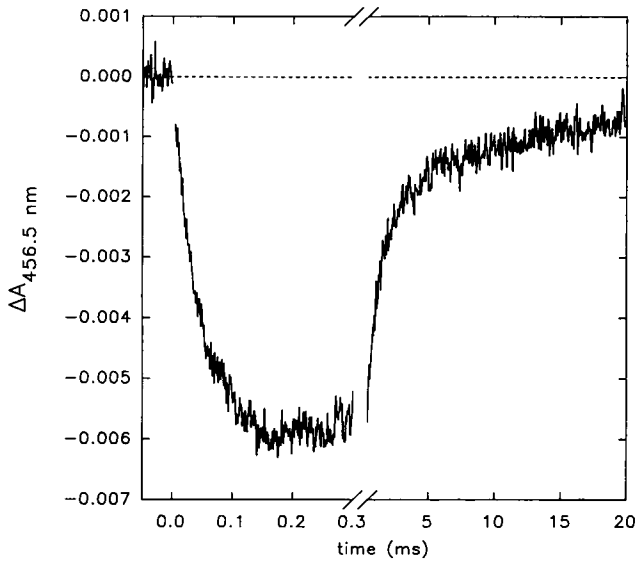

FIGURE 7 Dynamics of conformation changes after 92% photolysis of the sample from Fig. 6, observed at 456.5 nm. This wavelength is a deoxy/carbonmonoxy isosbestic point for the R state α chain (no initial absorbance change upon removal of CO). The rate of the slow phase of return to equilibrium (not complete at 20 ms) matches that of the slow phase of CO binding seen in Fig. 6.

studies, although the proportions of the two phases differ in each study (Cassoly and Gibson, 1972; Parkhurst et al., 1970), presumably because of differing solvent conditions. Indeed, solvent conditions are apparently the reason we do not find this biphasic, heterogeneous behavior for $\alpha^{+CN}\beta$, as was the case in the stopped-flow studies, because we do clearly see similar heterogeneous kinetics and "T-locked" material for $\alpha^{+CN}\beta$ in 0.1 M Tris, 0.1 M NaCl, pH 7.4 (data not shown).

To obtain further information about the allosteric kinetics of the rapid CO binding component, we have used two alternative procedures to subtract out the slowly combining component and then fitted the remainder to Scheme I. We first simply subtracted a single exponential of the correct rate and amplitude to eliminate the slow phase from the full photolysis data set. This procedure, however, in effect assumes that the slow binding component is generated instantaneously after photolysis and that this material exhibits no CO binding during the time ranges of R $\rightleftharpoons$ T equilibration or CO binding to R state material. As an alternative, because the slow component of this CN^- hybrid is very close in rate to the "T" binding phase of $\alpha\beta^{+aquo}$, in the second procedure we have subtracted a portion of the aquo hybrid kinetics sufficient to eliminate the slow phase in the CN^- hybrid kinetics. With this second assumption about half of the material has the slow CO binding behavior. Because the partial photolysis data showed no evidence for R $\rightarrow$ T switching, for these fits k_3^{RT} and k_3^{TR} were held fixed at 100 and 30,000 s^{-1}, respectively. Neither procedure for removing the slower component gave fits to the faster component that were entirely satisfactory, particularly with regard to consistency between data at different CO concentrations. Our best estimate is that k_2^{RT} = 4800 [3600, 7300] s^{-1} and k_2^{TR} = 3600 [3100, 6800] s^{-1}, where the best values and confidence intervals represent the mean results and the range of values obtained for the two subtraction techniques and/or with variation of other parameters as was done for other ferric ligands. Although there is a significant spread in these rates, this analysis supports the general picture that the faster component is material with an allosteric constant of ~1 and moderately fast R $\rightleftharpoons$ T kinetics, i.e., behavior consistent with extrapolating the results for other ligands to a form with $L_2 \approx 1$. The R $\rightleftharpoons$ T rates from this analysis are also consistent with the initial phase seen at the 456.5 nm isosbestic point (Fig. 7). Significantly, although the CO binding data seem to require a heterogeneity of allosteric kinetics, we do not see evidence for multiple components in this initial phase at 456.5 nm.

DISCUSSION

CO binding rates

One test of the validity of this complex data analysis is to ask whether the derived CO binding rates are in agreement with previous studies. We find l'_R = (5.6 ± 0.5) and (8 ± 0.8) × 10^6 M^{-1} s^{-1} for ferrous α and β, respectively. These values are in good agreement with values of 6–8 × 10^6 typically reported for the average of α and β (Sawicki and Gibson, 1978; Kwiatkowski and Noble, 1982; Hofrichter et al., 1983). They also agree with most estimates for the individual α and β rates (Sawicki and Gibson, 1976; Blough et al., 1980; Mathews et al., 1989; Blough and Hoffman, 1982), especially considering the differing solution conditions in different studies. (It also should be noted that it is often assumed to be identical to the rate seen for low levels of photolysis of HbCO. However, because it is now known that removal of a single ligand produces significant and moderately rapid switching to T (Zhang et al., 1990; Ferrone et al., 1985), some caution is necessary in interpreting earlier data where the R $\rightleftharpoons$ T dynamics have not been explicitly considered.) One exception to this agreement is the much lower value for the α chain derived from studies of site-directed mutants (Mathews et al., 1989). For the hybrid dimers, we find l'_{dimer} = (4.7 ± 0.3) and (5.3 ± 0.3) × 10^6 M^{-1} s^{-1} for α and β, in agreement with earlier estimates for average values for ferrous dimers (Gray, 1974, 1980) and chain-specific estimates from metal hybrid studies (Blough et al., 1980, 1984; Blough and Hoffman, 1984).

For the T state, we find l'_T = (8 ± 1) and (7 ± 1) × 10^4 M^{-1} s^{-1} for α and β. These values are in excellent agreement with the (7.5 ± 1.5) × 10^4 and (7.7 ± 1.6) × 10^4 M^{-1} s^{-1} $\alpha^+\beta$ averages reported for early stages of CO combination with Hb A by Hopfield et al. (1972) and Perrela et al.

(1992), respectively, and reasonable agreement with the 1×10^5 M^{-1} s^{-1} value from similar studies by Antonini et al. (1967). The l'_T values for individual chains from metal hybrid studies show a variation of ~50% depending on the metal substituted, and for the β chain, a reduction of ~3-fold in the presence of IHP, which suggests that l'_T is quite sensitive to structural details and solution conditions. Our values for α are, within error, the same as those reported for $\alpha^{Fe}\beta^{Zn}$ and $\alpha^{Fe}\beta^{Co}$, and for β they are only marginally slower than those for $\alpha^{Zn}\beta^{Fe}$ and $\alpha^{Co}\beta^{Fe}$ without IHP (Blough et al., 1980). Our T state rate constants are, however, considerably lower than those derived from studies of site-directed mutants (Mathews et al., 1991; Mathews and Olson, 1994), a difference that seems to arise because those studies found faster initial rates of CO binding to native deoxyHb A than have been reported by others (Hopfield et al., 1972; Perrella et al., 1992; Antonini et al., 1967).

In summary, we believe the CO association rates derived from our analysis are in good agreement with most earlier kinetic data. Furthermore, the values of these rates strongly suggest that the conformations we have labeled "R" and "T" in these valency hybrids are indeed the same as those of HbCO and deoxyHb, respectively.

R ⇌ T rates

For the various hybrids we find k_2^{RT} ranges from ~4,000 to 26,000 s^{-1}, i.e., values intermediate between ~50,000 s^{-1} for deoxyHb (Sawicki and Gibson, 1976; Murray et al., 1988) and ~1,500 s^{-1} for Hb with three bound CO's (Zhang et al., 1990). Thus one important result of this work is that we did not find the very slow R ⇌ T rates reported in other studies of diliganded Hb (Berjis et al., 1990; Sharma, 1988, 1989) for these valency hybrids (except, in part, for $\alpha\beta^{+CN}$).

A unique feature of these studies is having resolved the difference in structural kinetics produced by binding a single CO, and the ability to assess possible α/β differences. Earlier studies were fitted with models having k^{RT} reduced by a uniform factor of 2.4–4 per CO bound (Sawicki and Gibson, 1976; Marden et al., 1988). Our results show a stronger effect of ligation, with a reduction by 5 to 17 among $\alpha\beta^+$ hybrids and 8 to 20 among $\alpha^+\beta$ hybrids. Thus our results for CO are similar to those for O_2 by Sawicki and Gibson (1977b), who found a factor of 10 per O_2 bound.

This study also provides further support for a linear free energy relationship between quaternary rates and allosteric constants, as proposed by Eaton et al. (1991). All of the k_2^{RT} values in Table 1 fall close to the line they derived by fitting data primarily for unliganded or triply liganded Hb, even though these new data span a region of allosteric constants for which there were previously no data. The new k_3^{RT} values also are in reasonable agreement with this relationship, especially considering their fairly large uncertainties. Therefore we consider the present results to be a strong confirmation of this linear free energy model.

Allosteric constants and parameters

Table 2 summarizes the allosteric parameters for all of the hybrids, as calculated from the R ⇌ T rates. Although the uncertainties in many of the k_3^{RT} and k_3^{TR} values are fairly large, their ratio, L_3, is generally more precisely determined. The uncertainty in L_3 becomes fairly large when $L_2 > 100$ and is mainly due to that in k_3^{RT}. L_2 values for many of these same hybrids had previously been estimated from O_2 binding curves by Matsukawa et al. (1981). Our values agree within a factor of ~2, which is not unreasonable considering that some oxidation of the ferrous chains always occurs during O_2 binding studies, and the fact that to derive L from O_2 binding data in a system with two binding sites one must assume a value for either the R state binding affinity or c. Our L_2 values for the aquomet hybrids also agree with values of 70 ± 40 (Cordone et al., 1990) and 90 (Marden et al., 1991) from recent studies of O_2 binding to partially oxidized hemoglobin.

TABLE 2 Allosteric parameters

Hybrid type	L_2	L_3	$10^3 \times c$	% high spin in ferric subunit*
$\alpha\beta^{+F}$	340 (200, 700)	0.70 (.58 .83)	2.1 (1.2, 3.5)	95
$\alpha\beta^{+aquo}$	77 (65, 94)	0.14 (.06, .23)	1.8 (0.9, 2.8)	88
$\alpha\beta^{+SCN}$	540 (250, 800)	1.8 (1.6, 2.0)	3.3 (0.7, 7.0)	65
$\alpha\beta^{+azide}$	5.8 (5.3, 6.6)	0.034 (.001, .12)	6 (0.1, 9)	12
$\alpha\beta^{+CN}$	1.3 (.6, 2.1)‡	<0.03‡	—	0
$\alpha^{+F}\beta$	110 (90, 145)	0.16 (.05, .27)	1.4 (0.5, 2.2)	95
$\alpha^{+aquo}\beta$	95 (65, 120)	0.21 (.11, .30)	2.1 (1.3, 2.8)	88
$\alpha^{+SCN}\beta$	150 (120, 270)	0.76 (.60, .93)	5.1 (3.0, 6.2)	65
$\alpha^{+azide}\beta$	13 (10, 15)	0.08 (.02, .38)	6 (4, 30)	12
$\alpha^{+CN}\beta$	12 (9, 14)	0.10 (.02, .13)	8 (4, 14)	0

The allosteric constants were calculated from the R ⇌ T rates (Table 1), and the allosteric c from L_3/L_2.

*Average $\alpha+\beta$ subunit data for corresponding fully ferric Hb from Philo and Dreyer (1985); the actual values for α^+ or β^+ subunits in these hybrids may differ slightly from these values, but these values are consistent with the visible absorption spectra of the hybrids.

‡This hybrid is heterogeneous. Values listed are those for the component in rapid quaternary equilibrium, after subtracting the slow component (see text).

The data in Table 2 imply that CO (and presumably O_2) binding to these hybrids should be highly cooperative, with predicted Hill coefficients ranging from 1.4 to 1.8. (We are excluding from this discussion $\alpha(CO)\beta(CN^-)$, whose complex kinetic behavior makes it impossible to predict equilibrium properties.) The Hill coefficients reported for O_2 binding with a similar range of ferric ligands are 1.1 to 1.7 (Matsukawa et al., 1981), and 1.2 to 1.5 (Nagai, 1977), whereas 1.23 was recently found for the cyanomet forms only (Doyle and Ackers, 1992). Thus the O_2 binding Hill coefficients are in reasonable agreement with the present results.

The allosteric c parameter can be calculated from the ratio of L_3 to L_2. These values (Table 2) have a fairly large uncertainty, but they are consistent with the values of 2–10 $\times 10^{-3}$ generally found in an allosteric analysis of O_2 binding to Hb A under similar conditions (Matsukawa et al., 1981; Baldwin, 1975). The c values are the one area where our results differ significantly from those of Matsukawa et al. (1981), whose c values are as high as 0.3 for the N_3^- and CN^- hybrids. Their high c values would indicate a very small difference in R and T state binding affinities, and therefore a considerably distorted "R" or "T" state structure. The allosteric parameters of Mutsukawa et al. also imply that the N_3^- and CN^- hybrids will remain 20–45% in the T state when both ferrous subunits are liganded, which is inconsistent with both these kinetic data and NMR studies (Ogawa and Shulman, 1972).

α-β differences

These studies show a significant α-β difference in the variation of the allosteric equilibrium as the ferric ligand is changed. For $\alpha\beta^+$ the allosteric constants change by a factor of ~60 in going from fluoride to azide, whereas $\alpha^+\beta$ varies only ~8-fold. This pattern holds for both L_2 and L_3. Because of this difference the $\alpha\beta^+$ hybrids do not have a consistently higher or lower allosteric constant than their corresponding $\alpha^+\beta$ derivative.

The fact that we find L to be more sensitive to the type of ligand on β than that on α may reflect a more restricted environment distal to the heme in the β subunit, because the x-ray structures on T-state deoxy and aquomet Hb show that valine E11 and histidine E7 must move to accommodate the ferric ligand (Reisberg and Olson, 1980; Liddington et al., 1992). Given the marked α-β difference in sensitivity to the ferric ligand, it is remarkable that, within an uncertainty of ~2, no asymmetry is seen in c values, indicating that binding a CO to either α or β produces a similar change in the quaternary equilibrium.

A second type of asymmetry occurs in the rates of structural change. The R → T rates for the $\alpha\beta^+$ hybrids are always faster than those for the complementary $\alpha^+\beta$ hybrid. A third clear α-β asymmetry is seen in the tetramer → dimer dissociation, with the $\alpha^+\beta^{CO}$ hybrids always having greater dissociation than $\alpha^{CO}\beta^+$.

Changes in L with ferric ligand do not obey the predictions of the Perutz model

According to the Perutz stereochemical mechanism for cooperativity (Perutz, 1979), the quaternary equilibrium in Hb is governed solely by the coupling of changes in heme stereochemistry to the globin structure via the proximal histidine, and, reciprocally, the sole method through which the T structure lowers ligand binding affinity is by exerting "tension on the heme" through this proximal histidine linkage. Although the strict two-state allosteric formalism of this Perutz model is now known to be inadequate to explain oxygen binding equilibria in detail (Holt and Ackers, 1995; Ackers, 1990), this mechanism nonetheless still provides the fundamental basis of our understanding of the cooperative mechanism.

The changes in heme stereochemistry that are central to the Perutz mechanism are directly related to the spin state of the heme iron. For all of the ferric ligands we have studied, except cyanide, the ferric heme exists as an equilibrium between high-spin and low-spin forms. A low-spin ferric heme is a good stereochemical mimic of an oxy- or CO-liganded ferrous heme, whereas the high-spin ferric state more closely resembles a deoxy ferrous heme. Therefore, according to the Perutz model, those ferric ligands for which the heme spin state is predominantly high-spin should produce valency hybrids with larger allosteric constants. The present studies therefore allow us to test this prediction in detail.

The linkage between quaternary structure and the spin states of each ferric subunit can be quantitatively described by

$$\begin{array}{ccc} & \overset{K_s^R}{\rightleftharpoons} & \\ \text{(low spin, R)} & & \text{(high spin, R)} \\ L_{ls} \quad \downuparrows & & \quad \uparrow\downarrow \quad L_{hs}. \\ \text{(low spin, T)} & \underset{K_s^T}{\rightleftharpoons} & \text{(high spin, T)} \end{array} \qquad (2)$$

The strength of this coupling between the spin state and allosteric equilibria (the "tension on the heme") is then usually characterized by the "Perutz coupling energy" per heme, $\Delta\Delta G_{spin}$, which is given by

$$\Delta\Delta G_{spin} \equiv R \cdot T \cdot \ln(K_s^T/K_s^R) \equiv R \cdot T \cdot \ln([L_{hs}/L_{ls}]^{1/N}), \qquad (3)$$

where N is the number of ferric hemes per tetramer. It is important to note that as the ferric ligand is changed, the equilibrium between high- and low-spin forms is altered, but not the stereochemistry of the high-spin and low-spin states. Therefore the Perutz mechanism requires $\Delta\Delta G_{spin}$ to be the same for all ferric ligands.

Because we can neither directly observe the allosteric equilibrium for each pure spin state nor directly determine the spin equilibrium for a pure T state species, it is more useful to reformulate this coupling scheme as a function of

the overall allosteric equilibrium, L, the percentage of high-spin in the R state, and the coupling energy:

$$L = L_1 \cdot [1 + (e^{\Delta\Delta G_{spin}} - 1) \cdot (\%\ \text{high spin}, R)]. \quad (4)$$

This linkage model therefore predicts that L should be a linear function of the percentage high-spin. Based on the magnitude of the stereochemical differences between high- and low-spin ferric hemes versus those between deoxy- and oxy-ferrous hemes, the Perutz stereochemical model predicts a value for $\Delta\Delta G_{spin}$ of about 1000 cal/mol (Cho and Hopfield, 1979), which implies that L will be 31-fold higher for pure low-spin than for pure high-spin when there are two ferric hemes per tetramer. The "tension on the heme" may differ somewhat between the α and β subunits, and therefore the value of $\Delta\Delta G_{spin}$ may depend on which subunit is ferric, but $\Delta\Delta G_{spin}$ should be constant for all ferric ligands on the same type of subunit.

In Fig. 8 the variation of L with the percentage of high-spin in the ferric subunits (assumed to be that measured for the corresponding fully ferric form in the the absence of inositol hexaphosphate; Philo and Dreyer, 1985) is shown, as well as the behavior predicted from the Perutz model. The overall trend does show, as expected, that predominately high-spin ferric ligands produce higher allosteric constants, but in detail the data clearly deviate substantially from the quantitative predictions of the Perutz mechanism. Most significant is the absence of a linear dependence on the percentage high-spin (Eq. 4), but in addition we also find that the ratio L_{hs}/L_{ls} is smaller than predicted. These substantial deviations from the predictions of the Perutz mechanism occur no matter which type of subunit is ferric, and they are also observed when either zero or one CO is bound to the ferrous subunits.

These new results support our earlier magnetic studies of human methemoglobins (Philo and Dreyer, 1985), which also found neither the predicted magnitude of $\Delta\Delta G_{spin}$ nor the predicted constancy of $\Delta\Delta G_{spin}$ for different ferric ligands. A major difficulty in interpreting studies of methemoglobins is that, because they are always liganded, there is no way to obtain a functional assessment of their quaternary or allosteric state based on their ligand binding affinities. Therefore the magnetic studies relied on the original assignments by Perutz that certain human methemoglobins are converted completely from R to T in the presence of inositol hexaphosphate (Perutz et al., 1974, 1978). However, there is now evidence that this conversion from R to T is only partial, and thus the interpretation of the human metHb magnetic studies is open to question (Marden et al., 1991; Noble et al., 1989). These new data for valency hybrids provide a much better test of the Perutz mechanism, because the CO binding kinetics of the ferrous subunits serve as an unambiguous marker of the affinity state.

Although the Perutz model clearly fails to correctly predict the behavior of these valency hybrids, this does not necessarily imply that stereochemical changes at the heme do not play a major role in controlling quaternary transitions and regulating heme affinity. A key assumption of the Perutz model is that the only way that globin senses heme ligation is via the proximal histidine linkage. We have shown that certain ferric ligands affect the allosteric equilibrium much more or less than expected from their spin state (e.g., note the anomalously high allosteric constants for the SCN^- hybrids). This suggests that the protein conformation is sensing the ferric ligand through other modes in addition to the ligand's effects on spin state and heme stereochemistry. One likely possibility is that ligands are also sensed, and affinity regulated, through direct interactions with residues on the distal side of the heme pocket. Thus we think the proper conclusion from this analysis is not that the Perutz mechanism is fundamentally wrong, but rather that it is probably an incomplete description of the coupling of heme ligation to globin conformation.

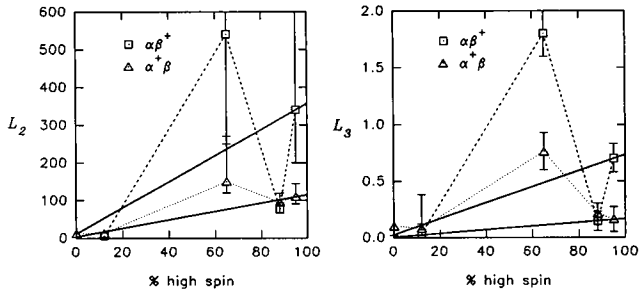

FIGURE 8 Allosteric constants versus percentage high spin of ferric subunits. The data points for each type of hybrid are connected by dashed or dotted lines to help identify the group to which they belong. According to the Perutz model, for each type of hybrid these data should fall on a straight line with the same ~30-fold difference in L_2 and L_3 in going from 0 to 100% high spin. The solid lines show the expected behavior for $\Delta\Delta G_{spin}$ = 1000 cal/mol, with L values selected to fit the F^- data for each hybrid.

Involvement of the R2/Y quaternary structure

Several years ago an alternative quaternary structure for liganded Hb was crystallized by two different groups and termed either the R2 (Silva et al., 1992) or Y (Smith and Simmons, 1994) structure. Furthermore, it has recently been argued that R2/Y is the correct structure for liganded Hb under physiological solvent conditions, and that the R structure is an intermediate between T and R2/Y that is trapped under the high-salt conditions used in crystallizing the R form (Srinivasan and Rose, 1994). It is certainly possible that the state we have called "R" in these studies is actually R2/Y. Furthermore, occupancy of (or transitions through) both R and R2/Y provides one possible explanation for the biphasic R → T kinetics we found for $\alpha\beta^{+SCN}$. It is also possible that as we change the ferric ligands, we are changing the equilibrium between R2/Y and R, either as a direct consequence of changing the heme ligand, or as an indirect

consequence of changing the ionic strength. However, we note that very similar quaternary dynamics were observed for the aquo- and fluoro-met hybrids, despite the fact that these represent the extremes of ionic strength, which suggests that there is no difference in their liganded quaternary structures.

Kinetics of formation of the "T locked" state in $\alpha^{+CN}\beta$

We have found that for $\alpha\beta^{+CN}$, as well as for $\alpha^{+CN}\beta$ at higher pH, a portion of the sample that we referred to as "T locked" (which we will hereafter call T* for simplicity) exhibits a very slow quaternary equilibrium, as seen in the early stopped-flow studies of the cyanomet hybrids (Cassoly and Gibson, 1972; Ogawa and Shulman, 1972; Parkhurst et al., 1970). Two important new results from this work are 1) a large portion of the sample is in a very rapid quaternary equilibrium (too rapid to have been seen in stopped-flow studies); and 2) despite the fact that full photolysis generates two populations with drastically different T → R rates, the initial R → T phase appears homogeneous.

The existence of a change from rapid to slow quaternary equilibria in similar partially liganded Hb species has, in fact, been reported previously. In stopped-flow studies of symmetric diliganded tetramers, Berjis et al. (1990) found that $(\alpha\beta^{CO})_2$ and $(\alpha^{CO}\beta)_2$ are initially capable of rapid R ⇌ T conversions, but then undergo a change to a slowly interconverting form. A similar conclusion was reached in pulsed radiolysis studies by Rollema et al. (1978). Therefore we postulate that immediately after photolysis all of the $\alpha\beta^{+CN}$ hybrid is in rapid R ⇌ T equilibrium (with rates as reported in Table 1), and that there is a subsequent T → T* conformational change, with T* only slowly interconverting with R. Our reinterpretation of the early stopped-flow studies is that the rapid binding "R" component is actually material in a rapid R ⇌ T equilibrium with an allosteric constant between ~1–10 (which also explains why the reported binding rates for the rapid component were slower than expected for a true R state), and the slow binding component in those studies is this T* state. Under our conditions the T → T* reaction is incomplete, either because the conformational equilibrium does not favor full occupation of T* or because of kinetic limitations (i.e., the T → T* rate may not be fast compared to CO binding). The fact that a pure slow binding phase is not seen even in stopped-flow studies, where the ferrous subunits are unliganded for long periods of time, probably indicates a T ⇌ T* equilibrium rather than a kinetic limitation (Cassoly and Gibson, 1972; Parkhurst et al., 1970).

It is not clear whether direct R ⇌ T* interconversion can occur, or instead whether T* is only formed via transitions with T. In Schemes II and III we show two models that are consistent with the available data. In Scheme II, k_4 must be slow to account for the slow overall T* → R conversion, and k_3 must therefore also be slow to maintain significant populations of both T and T*. A slow k_3 is consistent with our finding that larger amounts of T* are formed when the CO concentration is low, which allows more time for the T → T* conversion before CO binds. Under our conditions, however, k_3 must be faster than 20 s^{-1} to account for the T* we see. Scheme III, in which direct R ⇌ T* interconversions are allowed, is also consistent with the data if k_5 and k_6 as well as k_3 and k_4 are slow. We have not attempted any detailed analysis of the CO binding kinetics using either Scheme II or III, as there are simply too many unknown rates for a unique, meaningful analysis.

Nature of the T → T* change

The conformation we are calling T* is characterized by its slow interconversion with the R state. It is likely that this same T* state was seen in the double-mixing stopped-flow studies of diliganded Hb (Berjis et al., 1990; Sharma, 1988, 1989). T* therefore seems to occur in partially liganded tetramers with allosteric constants in the range 1–100, i.e., those where the presence of subunits in the liganded tertiary structure produces strain and destabilization of the T state. Therefore the T → T* transition is probably some conformation change that better accommodates the liganded subunits within the T structure, and its slow kinetics may indicate rearrangements in a large number of intersubunit contacts.

We suggest that for the symmetric cyanomet valency hybrids the T → T* transition may represent a spontaneous breaking of symmetry about the molecular diad, allowing a transition to an asymmetric state, with one deoxy subunit having low affinity and slow CO binding kinetics, and the other a high affinity and rapid binding. Berjis et al. (1990) have also suggested the coexistence of subunits with fast and slow CO binding kinetics within the T*-like state they observe for $(\alpha^{CO\beta})_2$ and $(\alpha\beta^{CO})_2$. The existence of asymmetric tetramers has also been proposed to explain the NMR

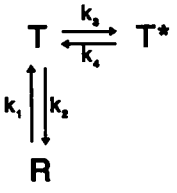

Scheme II

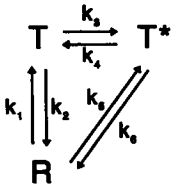

Scheme III

data for partially liganded (Miura and Ho, 1982) and asymmetrically modified cross-linked hemoglobins (Miura and Ho, 1984). High-affinity and low-affinity sites within an overall T structure are also now known to coexist for singly liganded Hb, where binding of a second ligand within the same $\alpha\beta$ dimer occurs with high affinity, but binding of a second ligand to the opposite dimer causes a change to the R state and therefore occurs with low affinity (Ackers et al., 1992). If, in fact, only one of the ferrous subunits in our T^* cyanomet hybrids has slow binding kinetics, then the fraction of T^* is ~50%.

Why does the $T \rightarrow T^*$ transition occur? The fact that initially the allosteric constant is ~1 shows that R and T are nearly isoenergetic, proving that there is considerable strain in trying to accommodate either two liganded subunits within an overall unliganded quaternary structure, or two unliganded subunits within an overall liganded quaternary structure. Therefore, one way to reduce the strain might be a spontaneous breaking of symmetry about the molecular diad. The slow interconversion with R and T of such an asymmetric state might then be a consequence of poor communication of structural changes across the dimer-dimer interface in such an asymmetric structure.

Whatever the precise nature of this T^* state, it is interesting that we clearly see the $T \rightarrow T^*$ transition only for cyanomet ferric subunits. We think it is likely that this difference among ferric ligands reflects the very strong Fe(III)-CN^- bond and the tight stereochemical restraints on the cyanomet heme. As noted previously, for all of the other ferric ligands we have studied, the ferric hemes exist as an equilibrium mixture of high- and low-spin forms, giving a more plastic heme-ligand geometry. This "softer" mixed-spin heme may allow these ferric subunits to be better accommodated within the normal T structure (as shown by the higher allosteric constants for the mixed-spin hybrids than for the cyanide hybrids), and therefore a transition to the T^* state may be energetically and/or kinetically less favorable for mixed-spin forms. Thus the $T \rightarrow T^*$ transition may be more favored in cyanomet hybrids as a way of satisfying the tight stereochemical restraints at cyanomet hemes while also maintaining most of the normal T state intersubunit contacts.

We would like to thank M. L. Adams and F. Safner for help with sample preparation and T. M. Schuster for encouragement, helpful discussions, and access to equipment.

This research was supported in part by grant HL-24644 from the National Institutes of Health; grants PCM 79-03964, 81-11320, and 82-11437 from the National Science Foundation; and the University of Connecticut Research Foundation. UD was supported in part by an E.M.B.O. postdoctoral fellowship.

REFERENCES

Ackers, G. K. 1990. The energetics of ligand-linked subunit assembly in hemoglobin require a third allosteric structure. *Biophys. Chem.* 37: 371–382.

Ackers, G. K., M. L. Doyle, D. Myers, and M. A. Daugherty. 1992. Molecular code for cooperativity in hemoglobin. *Science.* 255:54–63.

Antonini, E., M. Brunori, and S. Anderson. 1968. Studies on the relations between molecular and functional properties of hemoglobin. VII. Kinetic effects of the reversible dissociation of hemoglobin into single chain molecules. *J. Biol. Chem.* 243:1816–1822.

Antonini, E., E. Bucci, C. Fronticelli, J. Wyman, and A. Rossi-Fanelli. 1965. The properties and interactions of the isolated α and β chains of human haemoglobin. III. Observations on the equilibria and kinetics of the reactions with gases. *J. Mol. Biol.* 12:375–384.

Antonini, E., E. Chiancone, and M. Brunori. 1967. Studies on the relations between molecular and functional properties of hemoglobin. VI. Observations on the kinetics of hemoglobin reactions in concentrated salt solutions. *J. Biol. Chem.* 242:4360–4366.

Baldwin, J. M. 1975. Structure and function of haemoglobin. *Prog. Biophys. Mol. Biol.* 29:225–320.

Banerjee, R., F. Stetzkowski, and Y. Henry. 1973. Reciprocal effects of change of subunit structure on ligand equilibria of haemoglobin valency hybrids. Attempted correlation with electron paramagnetic resonance spectra. *J. Mol. Biol.* 73:455–467.

Berjis, M., D. Bandyopadhyay, and V. S. Sharma. 1990. Double-mixing kinetic studies of the reactions of methyl isocyanide and CO with diliganded intermediates of hemoglobin: $\alpha_2{}^{CO}\beta_2$ and $\alpha_2\beta_2{}^{CO}$. *Biochemistry.* 29:10106–10113.

Blough, N. V., and B. M. Hoffman. 1982. Equilibrium and kinetic CO binding parameters of T- and R-state hemoglobin chains using iron-manganese hybrids. *J. Am. Chem. Soc.* 104:4247–4250.

Blough, N. V., and B. M. Hoffman. 1984. Carbon monoxide binding to the ferrous chains of [Mn, Fe(II)] hybrid hemoglobins: pH dependence of the chain affinity constants associated with specific hemoglobin ligation pathways. *Biochemistry.* 23:2875–2882.

Blough, N. V., H. Zemel, and B. M. Hoffman. 1984. Flash photolytic studies of carbon monoxide binding to the ferrous chains of [Mn(II),Fe(II)] hybrid hemoglobins: kinetic mechanism for the early stages of hemoglobin ligation. *Biochemistry.* 23:2883–2891.

Blough, N. V., H. Zemel, B. M. Hoffman, T. C. K. Lee, and Q. H. Gibson. 1980. Kinetics of CO binding to manganese, zinc, and cobalt hybrid hemoglobins. *J. Am. Chem. Soc.* 102:5683–5685.

Brunori, M., G. Amiconi, E. Antonini, and J. Wyman. 1970. Artificial intermediates in the reaction of haemoglobin: functional and conformational properties of the cyanmet intermediates. *J. Mol. Biol.* 49:461–471.

Cassoly, R. 1981. Preparation of hemoglobin hybrids carrying different ligands: valency hybrids and related compounds. *Methods Enzymol.* 76:106–113.

Cassoly, R., and Q. H. Gibson. 1972. The kinetics of ligand binding to hemoglobin valency hybrids and the effect of anions. *J. Biol. Chem.* 247:7332–7341.

Cho, K. C., and J. J. Hopfield. 1979. Spin equilibrium and quaternary structure change in hemoglobin A. Experiments on a quantitative probe of the stereochemical mechanism of hemoglobin cooperativity. *Biochemistry.* 18:5826–5833.

Chu, A. H., and G. K. Ackers. 1981. Mutual effects of protons, NaCl, and oxygen on the dimer-tetramer assembly of human hemoglobin: the dimer Bohr effect. *J. Biol. Chem.* 256:1199–1205.

Cordone, L., A. Cupane, M. Leone, V. Militello, and E. Vitrano. 1990. Oxygen binding to partially oxidized hemoglobin: analysis in terms of an allosteric model. *Biophys. Chem.* 37:171–181.

Daugherty, M. A., M. A. Shea, J. A. Johnson, V. J. LiCata, G. J. Turner, and G. K. Ackers. 1991. Identification of the intermediate allosteric species in human hemoglobin reveals a molecular code for cooperative switching. *Proc. Natl. Acad. Sci. USA.* 88:1110–1114.

Doyle, M. L., and G. K. Ackers. 1992. Cooperative oxygen binding, subunit assembly, and sulfhydryl reaction kinetics of the eight cyanomet intermediate ligation states of human hemoglobin. *Biochemistry.* 31: 11182–11195.

Eaton, W. A., E. R. Henry, and J. Hofrichter. 1991. Application of linear free energy relations to protein conformational changes: the quaternary structural change of hemoglobin. *Proc. Natl. Acad. Sci. USA.* 88: 4472–4475.

Ferrone, F. A., A. J. Martino, and S. Basak. 1985. Conformational kinetics of triligated hemoglobin. *Biophys. J.* 48:269–282.

Gray, R. D. 1974. The effect of 2,3-diphosphoglycerate on the tetramer-dimer equilibrium of liganded hemoglobin. *J. Biol. Chem.* 249: 2879–2885.

Gray, R. D. 1980. The effect of H^+, inositol hexaphosphate, and Zn(II) on the tetramer-dimer equilibrium of liganded hemoglobin. *J. Biol. Chem.* 255:1812–1818.

Hofrichter, J., J. H. Sommer, E. R. Henry, and W. A. Eaton. 1983. Nanosecond absorption spectroscopy of hemoglobin: elementary processes in kinetic cooperativity. *Proc. Natl. Acad. Sci. USA.* 80: 2235–2239.

Holt, J. M., and G. K. Ackers. 1995. The pathway of allosteric control as revealed by hemoglobin intermediate states. *FASEB J.* 9:210–218.

Hopfield, J. J., S. Ogawa, and R. G. Shulman. 1972. The rate of carbon monoxide binding to hemoglobin Kansas. *Biochem. Biophys. Res. Commun.* 49:1480–1484.

Hopfield, J. J., R. G. Shulman, and S. Ogawa. 1971. An allosteric model of hemoglobin. I. Kinetics. *J. Mol. Biol.* 61:425–443.

Huang, Y., and G. K. Ackers. 1995. Enthalpic and entropic components of cooperativity for the partially ligated intermediates of hemoglobin support a "symmetry rule" mechanism. *Biochemistry.* 34:6316–6327.

Kwiatkowski, L. D., and R. W. Noble. 1982. The contribution of histidine (HC3) (146β) to the R state Bohr effect of human hemoglobin. *J. Biol. Chem.* 257:8891–8895.

LiCata, V. J., P. M. Dalessio, and G. K. Ackers. 1993. Single-site modifications of half-ligated hemoglobin reveal autonomous dimer cooperativity within a quaternary T tetramer. *Proteins.* 17:279–296.

Liddington, R., Z. Derewenda, E. Dodson, R. Hubbard, and G. Dodson. 1992. High resolution crystal structures and comparisons of T- state deoxyhaemoglobin and two liganded T-state haemoglobins: T(α-oxy)haemoglobin and T(met)haemoglobin. *J. Mol. Biol.* 228:551–579.

Makino, N., and Y. Sugita. 1982. The structure of partially oxygenated hemoglobin: a highly reactive intermediate toward a sulfhydryl titrant. *J. Biol. Chem.* 257:163–168.

Marden, M. C., E. S. Hazard, and Q. H. Gibson. 1986. Testing the two-state model: anomalous effector binding to human hemoglobin. *Biochemistry.* 25:7591–7596.

Marden, M. C., L. Kiger, J. Kister, B. Bohn, and C. Poyart. 1991. Coupling of ferric iron spin and allosteric equilibrium in hemoglobin. *Biophys. J.* 60:770–776.

Marden, M. C., J. Kister, B. Bohn, and C. Poyart. 1988. T-state hemoglobin with four ligands bound. *Biochemistry.* 27:1659–1664.

Marden, M. C., J. Kister, B. Bohn, and C. Poyart. 1991. Allosteric transition in triply met-haemoglobin. *J. Mol. Biol.* 217:303–306.

Mathews, A. J., and J. S. Olson. 1994. Assignment of rate constants for O_2 and CO binding to alpha and beta subunits within R- and T-state human hemoglobin. *Methods Enzymol.* 232:363–387.

Mathews, A. J., J. S. Olson, J.-P. Renaud, J. Tame, and K. Nagai. 1991. The assignment of carbon monoxide association rate constants to the α and β subunits in native and mutant human deoxyhemoglobin tetramers. *J. Biol. Chem.* 266:21631–21639.

Mathews, A. J., R. J. Rohlfs, J. S. Olson, J. Tame, J. P. Renaud, and K. Nagai. 1989. The effects of E7 and E11 mutations on the kinetics of ligand binding to R state human hemoglobin. *J. Biol. Chem.* 264: 16573–16583.

Matsukawa, S., K. Mawatari, and Y. Yoneyama. 1981. Close correlation between Monod-Wyman-Changeux parameters, L and c, and its implication for the stereochemical mechanism of haemoglobin allostery. *J. Mol. Biol.* 150:615–621.

Mawatari, K., S. Matsukawa, and Y. Yoneyama. 1983. Spectral changes upon subunit association in valency hybrid hemoglobins. *Biochim. Biophys. Acta.* 748:381–388.

Mawatari, K., S. Matsukawa, Y. Yoneyama, and Y. Takeda. 1987. Assessment of the $\alpha_1\beta_2$ contact structure of valency hybrid hemoglobins by ultraviolet difference spectra. *Biochim. Biophys. Acta.* 913:313–320.

Miura, S., and C. Ho. 1982. Preparation and proton nuclear magnetic resonance investigation of cross-linked mixed valency hybrid hemoglobins: models for partially oxygenated species. *Biochemistry.* 21:6280–6287.

Miura, S., and C. Ho. 1984. Proton nuclear magnetic resonance investigation of cross-linked asymmetrically modified hemoglobins: influence of the salt bridges on tertiary and quaternary structures of hemoglobin. *Biochemistry.* 23:2492–2499.

Miura, S., M. Ikeda-Saito, T. Yonetani, and C. Ho. 1987. Oxygen equilibrium studies of cross-linked asymmetrical cyanomet valency hybrid hemoglobins: models for partially oxygenated species. *Biochemistry.* 26:2149–2155.

Morishima, I., M. Hara, and K. Ishimori. 1986. Interaction of fully liganded valency hybrid hemoglobin with inositol hexaphosphate. Implication of the IHP-induced T state of human adult methemoglobin in the low-spin state. *Biochemistry.* 25:7243–7250.

Morris, R. J., Q. H. Gibson, M. Ikeda-Saito, and T. Yonetani. 1984. Geminate combination of oxygen with iron-cobalt hybrid hemoglobins. *J. Biol. Chem.* 259:6701–6703.

Murray, L. P., J. Hofrichter, E. R. Henry, and W. A. Eaton. 1988. Time-resolved optical spectroscopy and structural dynamics following photodissociation of carbonmonoxyhemoglobin. *Biophys. Chem.* 29:63–76.

Nagai, K. 1977. The effect of ferric ligands on the oxygen affinity of the ferrous subunits in valency hybrid haemoglobins. *J. Mol. Biol.* 111: 41–53.

Nagel, R. L., and Q. H. Gibson. 1972. The hemoglobin-haptoglobin reaction as a probe of hemoglobin conformation. *Biochem. Biophys. Res. Commun.* 48:959–966.

Noble, R. W., A. DeYoung, S. Vitale, M. Cerdonio, and E. E. DiIorio. 1989. Spin equilibria in human methemoglobin: effects of bezafibrate and inositol hexaphosphate as measured by susceptometry and visible spectroscopy. *Biochemistry.* 28:5288–5292.

Ogawa, S., and R. G. Shulman. 1972. High resolution nuclear magnetic resonance spectra of hemoglobin. III. The half-ligated state and allosteric interactions. *J. Mol. Biol.* 70:315–336.

Olson, J. S., R. J. Rohlfs, and Q. H. Gibson. 1987. Ligand recombination to the alpha and beta subunits of human hemoglobin. *J. Biol. Chem.* 262:12930–12938.

Parkhurst, L. J., G. Geraci, and Q. H. Gibson. 1970. Kinetics of the reaction of hybrid-heme hemoglobins with carbon monoxide. *J. Biol. Chem.* 245:4131–4135.

Perrella, M., A. Colosimo, L. Benazzi, M. Ripamonti, and L. Rossi-Bernardi. 1990. What the intermediate compounds in ligand binding to hemoglobin tell about the mechanism of cooperativity. *Biophys. Chem.* 37:211–223.

Perrella, M., N. Davids, and L. Rossi-Bernardi. 1992. The association reaction between hemoglobin and carbon monoxide as studied by the isolation of intermediates. *J. Biol. Chem.* 257:8744–8751.

Perutz, M. F. 1979. Regulation of oxygen affinity in hemoglobin: influence of structure of the globin on the heme iron. *Annu. Rev. Biochem.* 48:327–386.

Perutz, M. F., A. R. Fersht, S. R. Simon, and G. C. K. Roberts. 1974. Influence of globin structure on the state of the heme. II. Allosteric transitions in methemoglobin. *Biochemistry.* 10:2174–2186.

Perutz, M. F., J. K. M. Sanders, D. H. Chenery, R. W. Noble, R. R. Pennelly, L. W.-M. Fung, C. Ho, I. Giannini, D. Porschke, and H. Winkler. 1978. Interactions between the quaternary structure of the globin and spin state of the heme in ferric mixed spin derivatives of hemoglobin. *Biochemistry.* 17:3640–3662.

Philo, J. S., M. L. Adams, and T. M. Schuster. 1981. Association-dependent absorption spectra of oxyhemoglobin A and its subunits. *J. Biol. Chem.* 256:7917–7924.

Philo, J. S., and U. Dreyer. 1985. Quaternary structure has little influence on spin-states in mixed-spin human methemoglobins. *J. Biol. Chem.* 263:682–689.

Philo, J. S., J. W. Lary, and T. M. Schuster. 1988. Quaternary interactions in hemoglobin beta subunits: kinetics of ligand binding and self-assembly. *J. Biol. Chem.* 263:682–689.

Reisberg, P. I., and J. S. Olson. 1980. Kinetic and cooperative mechanisms of ligand binding to hemoglobin. *J. Biol. Chem.* 255:4159–4169.

Rollema, H. S., A. Raap, and S. H. de Bruin. 1978. Kinetics of carbon monoxide binding to fully and partially reduced human hemoglobin valency hybrids. *Eur. J. Biochem.* 83:313–317.

Sawicki, C. A., and Q. H. Gibson. 1976. Quaternary conformational changes in human hemoglobin studied by laser photolysis of carboxyhemoglobin. *J. Biol. Chem.* 251:1533–1542.

Sawicki, C. A., and Q. H. Gibson. 1977a. Properties of the T state of human oxyhemoglobin studied by laser photolysis. *J. Biol. Chem.* 252: 7538–7547.

Sawicki, C. A., and Q. H. Gibson. 1977b. Quaternary conformational changes in human oxyhemoglobin studied by laser photolysis. *J. Biol. Chem.* 252:5783–5788.

Sawicki, C. A., and Q. H. Gibson. 1978. The relation between carbon monoxide binding and the conformational change of hemoglobin. *Biophys. J.* 24:21–33.

Sharma, V. S. 1988. Kinetic studies on partially liganded species of carboxyhemoglobin: $\alpha_2^{CO}\beta_2$ and $\alpha_2\beta_2^{CO}$. *J. Biol. Chem.* 263: 2292–2298.

Sharma, V. S. 1989. Kinetic studies on partially liganded species of carboxyhemoglobin: $(\alpha_1^{CO}\beta_1^{CO})\alpha_2\beta_2$ or $(\alpha_2^{CO}\beta_2^{CO})\alpha_1\beta_1$. *J. Biol. Chem.* 264:10582–10588.

Sharma, V. S., M. R. Schmidt, and H. M. Ranney. 1976. Dissociation of CO from carboxyhemoglobin. *J. Biol. Chem.* 251:4267–4272.

Shibayama, N., T. Inubushi, H. Morimoto, and T. Yonetani. 1987. Proton nuclear magnetic resonance and spectrophotometric studies of nickel(II)-iron(II) hybrid hemoglobins. *Biochemistry.* 26:2194–2201.

Silva, M. M., P. H. Rogers, and A. Arnone. 1992. A third quaternary structure of human hemoglobin A at 1.7-Å resolution. *J. Biol. Chem.* 267:17248–17256.

Smith, F. R., D. Gingrich, B. M. Hoffman, and G. K. Ackers. 1987. Three-state combinatorial switching in hemoglobin tetramers: comparison between functional energetics and molecular structures. *Proc. Natl. Acad. Sci. USA.* 84:7089–7093.

Smith, F. R., E. E. Lattman, and C. W. Carter, Jr. 1991. The mutation β99 Asp-Tyr stabilizes Y: a new, composite quaternary state of human hemoglobin. *Proteins.* 10:81–91.

Smith, F. R., and K. C. Simmons. 1994. Cyanomet human hemoglobin crystallized under physiological conditions exhibits the Y quaternary structure. *Proteins.* 18:295–300.

Srinivasan, R., and G. D. Rose. 1994. The T-to-R transformation in hemoglobin: a reevaluation. *Proc. Natl. Acad. Sci. USA.* 91: 11113–11117.

Tentori, L., and A. M. Salvati. 1981. Hemoglobinometry in human blood. *Methods Enzymol.* 76:707–715.

Tomoda, A., M. Takeshita, and Y. Yoneyama. 1978a. Characterization of intermediate hemoglobin produced during methemoglobin reduction by ascorbic acid. *J. Biol. Chem.* 253:7415–7419.

Tomoda, A., A. Tsuji, S. Matsukawa, M. Takeshita, and Y. Yoneyama. 1978b. Mechanism of methemoglobin reduction by ascorbic acid under anaerobic conditions. *J. Biol. Chem.* 253:7420–7423.

Turner, B. W., D. W. Pettigrew, and G. K. Ackers. 1981. Measurement and analysis of ligand-linked subunit dissociation equilibria in human hemoglobins. *Methods Enzymol.* 76:596–628.

Unno, M., K. Ishimori, I. Morishima, T. Nakayama, and K. Hamanoue. 1991. Pressure effects on carbon monoxide rebinding to the isolated α and β chains of human hemoglobin. *Biochemistry.* 30:10679–10685.

Zhang, N., F. A. Ferrone, and A. J. Martino. 1990. Allosteric kinetics and equilibria differ for carbon monoxide and oxygen binding to hemoglobin. *Biophys. J.* 58:333–340.